



3 1176 00156 6968

NASA CR-159,161

## NASA Contractor Report 159161

NASA-CR-159161

19800002792

LEADING EDGE VORTEX-FLAP EXPERIMENTS ON A  
74 DEG. DELTA WING

Dhanvada M. Rao

OLD DOMINION UNIVERSITY RESEARCH FOUNDATION  
Norfolk, Virginia 23508

LIBRARY COPY

NASA Grant NSG-1315  
November 1979

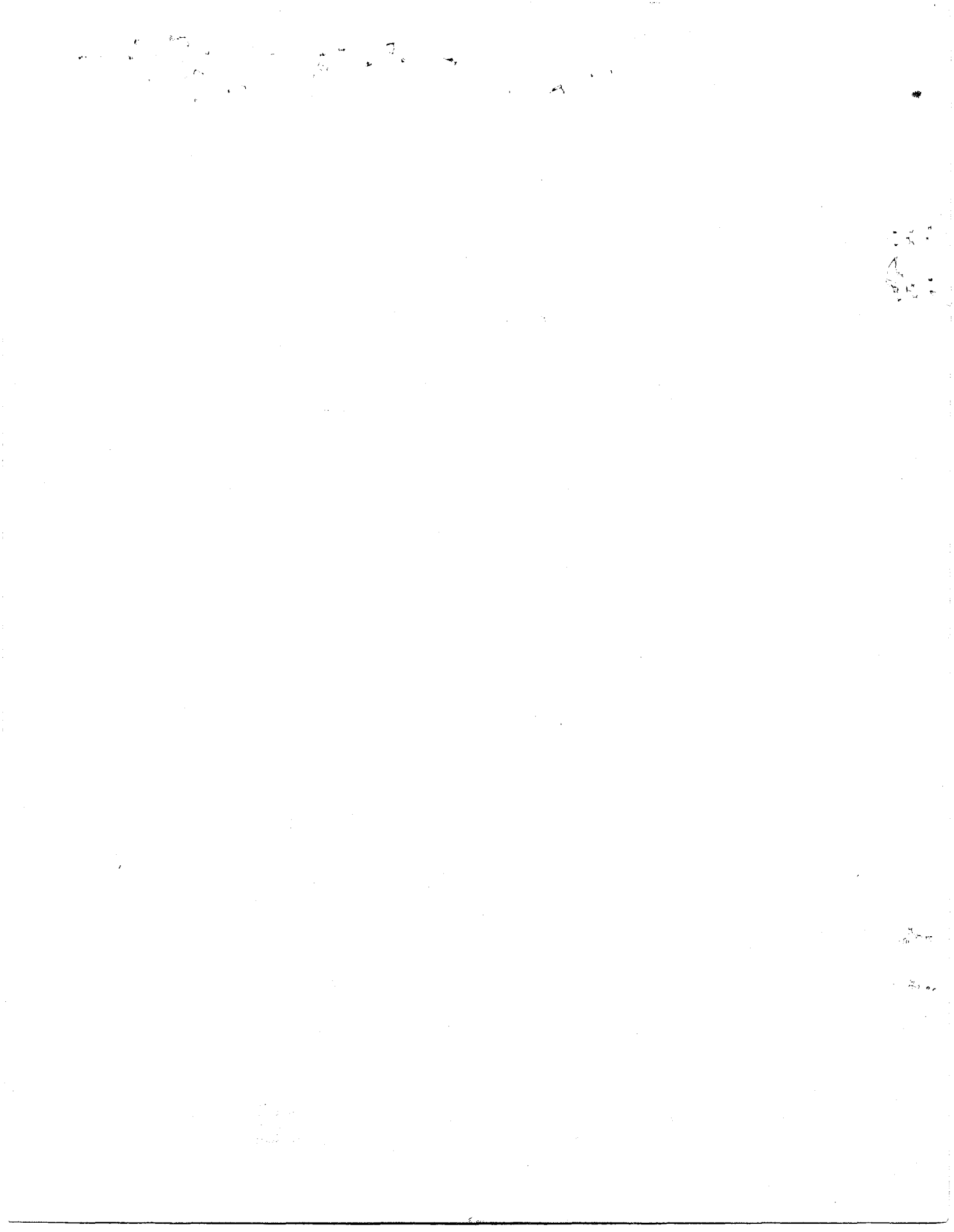
NOV 27 1979

LANGLEY RESEARCH CENTER  
LIBRARY, NASA  
HAMPTON, VIRGINIA



National Aeronautics and  
Space Administration

**Langley Research Center**  
Hampton, Virginia 23665



# LEADING EDGE VORTEX-FLAP EXPERIMENTS ON A 74 DEG. DELTA WING\*

Dhanvada M. Rao<sup>+</sup>  
Old Dominion University Research Foundation

## ABSTRACT

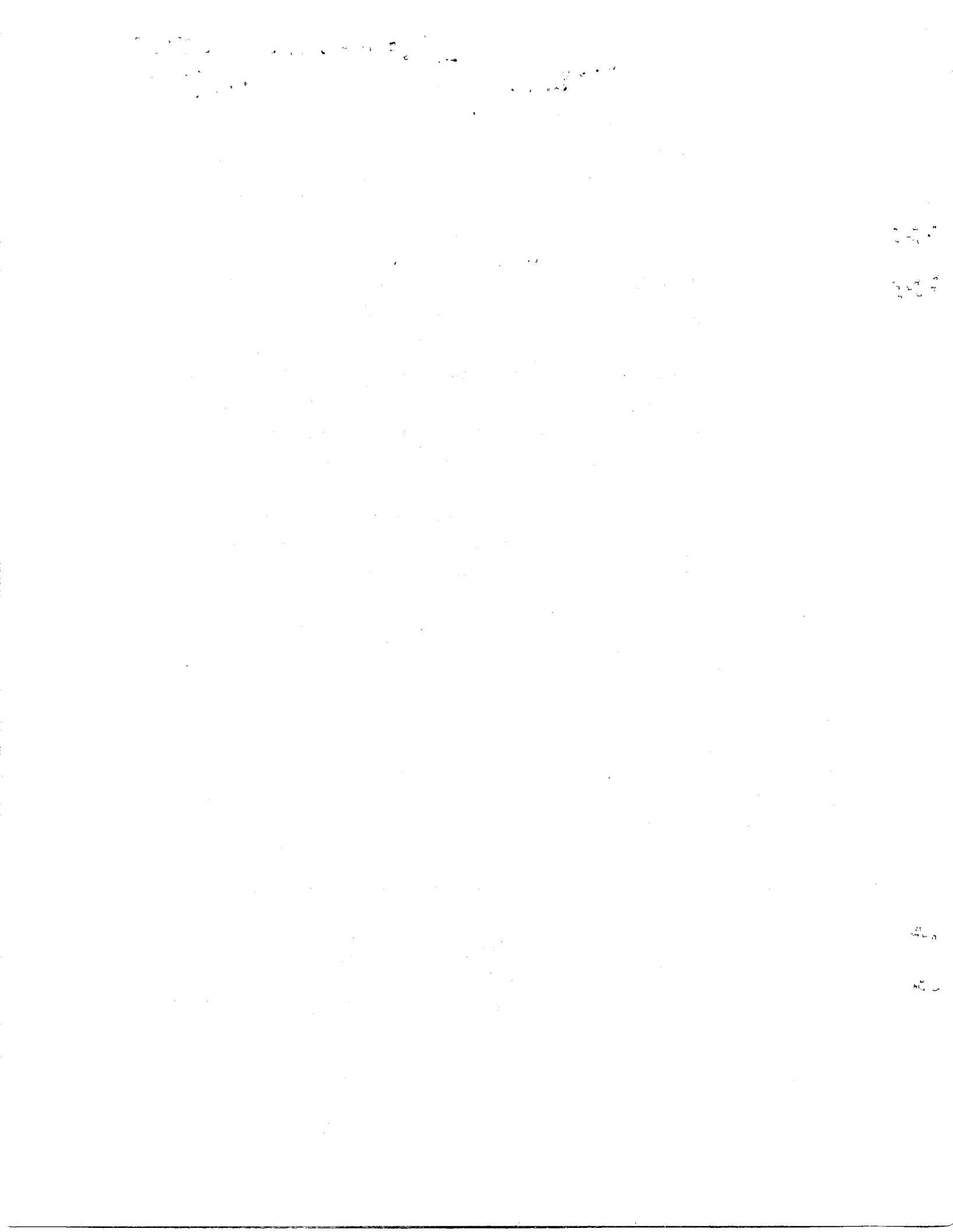
Exploratory wind-tunnel tests are reported on a 74 deg. delta wing model to evaluate the potential of a vortex-flap concept in reducing the subsonic lift-dependent drag of highly swept, slender wings. The concept utilizes the suction effect of coiled vortices generated through controlled separation over leading-edge flap surfaces to produce a thrust component. A series of vortex-flap configurations were investigated to explore the effect of some primary geometric variables. The most promising flap arrangement produced drag reductions in excess of 30% relative to the basic wing in the range of lift coefficient 0.4 to 0.8.

---

\* Research supported by NASA Grant No. NSG-1315.

+ Research Associate, ODURF and Research Professor, Dept. of Mechanical Engineering and Mechanics, Old Dominion University, Norfolk, Virginia.

N80-11038 #



## INTRODUCTION: THE VORTEX-FLAP CONCEPT

Extensive research in recent years on highly swept, slender wings for supersonic cruise aircraft has revealed serious performance, stability and control deficiencies in the subsonic, high-lift flight regime. Leading-edge flow separation and the consequent loss of leading-edge suction on such wings is responsible for large increases in drag even at moderate angles of attack, while the resultant formation of concentrated vortices on the wing induces undesirable stability and handling characteristics (for example, see ref. 1).

Leading-edge flaps have commonly been employed on wings of moderate sweep angle in order to maintain attached flow to higher angles of attack. However, on low aspect-ratio wings with leading-edge sweep exceeding 70 deg. as found on typical supersonic cruise planforms (such as the delta and arrow wings), this approach appears to be less practical. The circulation-induced upwash angle at the leadings edges of such wings rapidly attains high values with increasing angle of attack (when viewed in the plane normal to the leading edge), and also varies appreciably in the spanwise direction. In such cases, the large flap deflections needed may only succeed in moving the position of separation from the leading edge to the knee-line which will nullify some of the drag benefit, while the vortex flow will still persist over the wing. (see fig. 1, C).

The leading-edge vortex-flap concept (fig. 1, D) offers an alternative to the conventional attached-flow approach for drag reduction on highly swept wings. Through controlled separation at the flap leading edges, coiled vortices are generated whose suction effect over the forward-sloping flap surfaces provides a thrust component. The high degree of leading-edge sweep enhances the stability and persistence of the vortices along the flap length. For the vortex suction peak to be maintained on the flap, it would in-

tuitively appear necessary for the vortex-induced attachment of the inviscid (dividing) streamline to occur on the flap surface. An adequate flap chord is therefore essential in consideration of the vortex core size and also to accommodate the inboard movement of the core with increasing angle of attack. On a conventional leading-edge flap which essentially forms a part of the main wing surface, moving the hinge-line inboard in order to enlarge the flap chord will be limited by structural as well as aerodynamic considerations, particularly so on slender planforms. Accordingly, auxiliary surfaces that extend out of the basic wing appear to be the most effective means of exploiting the vortex-flap concept.

The most efficient operation of the vortex-flap would be expected to occur when the induced attachment is just at the leading edge, as indicated in fig. 1, D. This condition not only will bring the entire flap chord under vortex suction but also favor a smooth flow entry to the wing. To obtain this optimum flow pattern simultaneously at all spanwise sections will in general require a varying flap angle according to the prevailing upwash distribution. In the interest of retaining the basic simplicity of the vortex-flap concept, however, constant flap deflection and simple chord variation (such as constant taper) only have been considered in this preliminary study.

This report presents the results of an exploratory wind-tunnel evaluation of the vortex-flap applied to a 74 deg. flat delta wing at a subsonic Mach number. The primary objectives of this study were to improve the aerodynamic efficiency of the basic delta wing by means of simple vortex-flap arrangements in the lift-coefficient range 0.4 to 0.8, and in the process to obtain an insight into the relative importance of some of the primary geometric variables of the vortex-flaps.

## LIST OF SYMBOLS

A	Aspect ratio
$\bar{c}$	Mean aerodynamic chord (m.a.c.) of basic wing
$C_A$	Axial force coefficient
$C_{D_L}$	Lift-dependent drag coefficient ( $= C_D \text{total} - C_D \text{zero-lift}$ )
$C_L$	Lift coefficient (on basic wing reference area)
$C'_L$	Lift coefficient (on total projected plan area, including LEVF)
$C_m$	Pitching moment coefficient
$C_N$	Normal force coefficient
$C_T$	Leading-edge thrust coefficient
$d_{H.L.}$	Distance of LEVF hinge line, normal to leading edge
L/D	Lift-to-drag ratio
S	Basic wing area
$S'$	Total projected plan area, including LEVF
$\alpha$	Angle of attack
$\delta_L$	LEVF deflection angle in the plane normal to hinge line
$\delta_T$	Trailing-edge flap deflection

## ABBREVIATIONS USED IN TABULATED DATA

ALPHA	Angle of attack
CD	Drag coefficient
CL	Lift coefficient
CMS	Pitching moment coefficient
CRMS	Rolling moment coefficient
CYMS	Yawing moment coefficient
CYS	Side force coefficient
MACH	Free-stream Mach number
Q	Free-stream dynamic pressure

(Note: Moments are referred  
to wind axes)

## MODELS AND TEST DETAILS

The basic wing was an existing  $74^{\circ}$  delta model previously tested with sharp leading edges (ref. 2). For the present investigation, the leading edges were modified to a constant-radius (0.635 cm), semi-circular cross section (fig. 2). The flaps were cut from 0.16 cm thick aluminum sheet, bent as required and fastened to the wing lower surface with screws. The model had a fuselage-like integral housing for a six-component strain-gage balance.

The following LEVF configurations were tested (fig. 3):

LEVF I - Full-span, constant chord flaps joined ahead of the wing apex. Starting with this initial arrangement, increasing portions of the flap from the apex (25, 50 and 75 percent of the leading-edge length) were successively cut off along a chordwise line to generate the partial-flap series.

LEVF II - Modification of (I) with the 25-percent length removed along a swept-back (rather than chordwise) line.

LEVF III - Modification of (II) to generate an inverse-taper flap.

LEVF IV - Extended-flap obtained by attaching a flat extension to (III) projecting inboard over the wing.

The dimensions of the various flap configurations are given in fig. 4. The tests were carried out in the NASA Langley 7-by 10-foot high speed tunnel at a nominal Mach number of 0.2 and a Reynolds number of  $2.75 \times 10^6$  based on the mean aerodynamic chord.

## DATA PRESENTATION

The emphasis in this study was on the performance potential of the LEVF concept. Accordingly, the graphical presentation of the results in this report consist mainly of L/D plotted versus lift coefficient. Some additional analysis plots are also included as needed to support the discussion of results. The wind-tunnel test schedules and tabulated balance data are included in Appendix at the end of the report.

### DISCUSSION OF RESULTS

For a ready evaluation of the LEVF drag-reduction potential, the flaps-on L/D versus  $C_L$  characteristics will be compared with the flaps-off (basic wing) data. Noting that the basic wing of the present study had blunt leading edges, a further comparison will be offered by including the sharp leading edge data taken from ref. 2. The relatively large leading-edge radius on the present basic wing (amounting to approximately 1-percent of  $c$ ) is unrepresentative of supersonic wings, and it may therefore be more appropriate to use the sharp leading edge results as the baseline. At lift coefficients greater than about 0.6 the basic wing L/D is virtually the same with either sharp or blunt leading edges (and corresponds to zero leading-edge suction case).

Since the basic wing reference area ( $S$ ) has been employed in deriving the lift coefficients, a part of the LEVF benefit apparent in the L/D vs.  $C_L$  comparisons will be due to the planform area increase from the flaps. It is quite legitimate to take advantage of this effect since area-increase is an essential part of the present LEVF concept (see INTRODUCTION). However, in order to appreciate the relative aerodynamic effectiveness of the various LEVF test configurations with different amounts of flap area, the L/D data have also been plotted against  $C'_L = C_L \cdot S/S'$  where  $S'$  is the total projected plan area including the LEVF.

#### Constant Chord, Full Span LEVF I

In a practical installation the LEVF will be hinged some distance behind the leading edge for structural reasons. The hinge-line positions investigated are defined in fig. 2. The effect of increasing hinge distance behind the leading edge was found detrimental to LEVF performance (figs. 5A and 6A), even on the area-corrected basis (figs. 5B and 6B). These results suggest that the leading-edge overhang has an adverse influence on the formation and stability of the flap vortex.

The effect of varying the flap deflection from  $30^\circ$  to  $45^\circ$  at a constant hinge-line position is shown in fig. 7A. When the corresponding variation in the projected area is taken into consideration, the LEVF performance is found to be virtually identical at the two deflection angles for  $C_L > 0.4$  (fig. 7B). The adverse effect noted in the  $45^\circ$  flap data at the lower lift coefficients indicates that in this range the flap is effectively over-deflected, resulting in separation and vortex formation on the lower surface of the flap with a corresponding drag penalty.

#### Constant-Chord, Part-Span LEVF I

The part-span LEVF configurations were of interest because they appeared to be more practical for aircraft applications where a fuselage would be present. Also, it was anticipated that the forward portions of the vortex-flaps would be relatively less effective due to the low upwash angles encountered closer to the wing apex. The effect of progressive flap length cut-off from the apex is shown in fig. 8A. On area-corrected basis, removal of the first 25-percent of the flap was found to produce virtually no loss in performance within the  $C_L$  range of interest, while actually showing some improvement at lower lift coefficients (fig. 8B).

#### Constant Chord, Part Span LEVF II

Removing the first 25-percent of the flap along a swept-back line (as opposed to the chordwise cut of LEVF I) results in a much improved performance as shown in fig. 9, particularly at the lower lift coefficients. Remarkably, this LEVF modification at  $30^\circ$  deflection even raises the  $(L/D)_{max}$  above the basic-wing value. Also, the drag penalty at the lower lift coefficients with  $45^\circ$  flap angle (noted in case of LEVF I) is considerably alleviated.

#### Comparison of LEVF II and LEVF III

The constant-chord LEVF II is compared with the inverse-taper flap for  $30^\circ$  deflection in fig. 10. LEVF III was generated by removing material from LEVF II and as a consequence was about 20-percent smaller in area; nevertheless, it produces nearly the same

performance in the  $C_L$  range of interest. This improved efficiency of LEVF III is not surprising since the inverse taper was intended to accommodate the spanwise expansion of the flap vortex.

#### Extended Flap, LEVF IV

A method of increasing the effective chord of the vortex-flap to insure vortex 'capture' at higher at higher angles of attack (but without incurring excessive hinge moments) is illustrated in fig. 11. An additional flap is provided on the upper surface of the wing and deployed such that it forms a virtual extension of the lower flap. The upper-surface flap will necessarily produce a large separated-flow region with a corresponding drag penalty. However, it was surmised that the separation occurring along a highly swept edge would result in a coiled vortex type flow behind the upper flap. The entrainment effect would then energize the lee-side flow on the wing specially at high angles of attack and thus provide compensating benefits such as improved trailing-edge flap effectiveness.

On the test model a flat-plate flap was mounted across either leading edge to simulate a  $30^\circ$  extended flap configuration. The inner edges of the plates were bent up in a  $45^\circ$  lip in an attempt to increase the velocity at separation and thereby intensify the inboard vortices. Smoke visualization at low speed with this model confirmed the presence of these vortices at angles of attack greater than about  $5^\circ$  (fig. 12).

The lift curves of LEVF III and LEVF IV are compared in figs. 13 A and 13 B. Noteworthy is the additional lift on the extended flap configuration over a substantial angle-of-attack range. It seems reasonable to attribute the lift increment to the suction effect of the inboard vortices. The L/D data show the relatively large drag penalty incurred with LEVF IV at the lower lift coefficients (fig. 14). However, between  $C_L = 0.5$  and 0.8 the extended flap performs better than LEVF III, or equally well on the area-corrected basis. The performance advantage of LEVF IV at

higher  $C_L$ 's appears to stem largely from it's better lift characteristics. These results although limited to a single geometry and one deflection angle, appear sufficiently interesting to warrant further study of the extended flap concept, particularly to develop it's unique lift-enhancing capability.

#### Effect of Trailing-Edge Flaps

Slender wing configurations typically have reduced lift-curve slopes which dictates the use of trailing-edge flaps in order to attain high lift coefficients for take off and landing. As shown in fig. 15, trailing-edge flaps produce L/D improvements on the basic wing by allowing angle-of-attack reduction for a given lift coefficient. Such improvements are found also on the wing with leading-edge vortex-flaps present (fig. 16).

The trailing-edge flap effectiveness at  $\delta_T = 30^\circ$  measured in terms of lift and pitching-moment increments relative to  $\delta_T = 0^\circ$  is shown in fig. 17 for different LEVF configurations over the angle of attack range. A rise in  $\Delta C_L$  beginning at about  $6^\circ$  angle of attack on the basic wing is attributed to the onset of leading-edge vortices which entrain high dynamic pressure flow on the lee side. By comparison, the LEVF III data suggest that vortex formation over the wing was delayed to a much higher angle of attack. With extended flaps, a significantly higher lift increment due to trailing-edge flap deflection is evident throughout the angle of attack range. This again may be attributed to the entrainment effect of the inboard vortices unique to this flap configuration.

#### Longitudinal Stability

At a constant LEVF deflection, increasing angle of attack results in a forward movement of the vortex origin along the flaps due to the characteristic spanwise development of the leading-edge upwash. Accordingly, a longitudinal shift of the center of pressure may be anticipated. Pitching-moment data for the three LEVF configurations presented in fig. 18 indicate a reduction

in stability compared to the basic wing at angles of attack below about  $10^\circ$ , as expected from the flap area addition forward of the moment center. At higher angles of attack, however, when the whole length of the flap is under vortex flow (as confirmed by oil flow visualizations), there is an increase of the  $C_m$ -slope to the same level as on the basic wing. With LEVF III, the pitching moments above  $18^\circ$  angle of attack are nearly identical with the basic-wing data, suggesting that the flap vortices have moved inboard on to the wing.

#### Vortex-Flap Thrust Characteristics

Although the lift/drag ratio comparisons discussed previously are convenient for the purpose of assessing the relative performance of vortex-flap configurations, the magnitude of L/D are based on the total drag characteristics of an idealised test model at the wind-tunnel test Reynolds number and therefore quite un-representative of the flight vehicle. The drag-reduction due to vortex-flaps may be more directly evaluated by a study of the effective thrust generated by the flaps. This was attempted by using the axial-force balance measurements which provide a sensitive and direct indication of the aerodynamic thrust.

Typical axial-force coefficient data are plotted versus angle of attack for the basic wing as well as the LEVF configurations in fig. 19. With increasing angle of attack the axial force steadily decreases and becomes negative as the leading-edge thrust overcomes the combined axial force due to skin friction, pressure drag from trailing-edge separation, balance-housing drag and base drag. The axial-force coefficient with LEVF on starts with a much higher positive value at zero angle of attack but rapidly attains negative values considerably in excess of those obtained on the basic wing, indicating the powerful thrust effect of the vortex-flaps. Of the three flap configurations compared in fig. 19 the inverse-taper LEVF III alone shows a distinct axial-force break (at approximately  $17^\circ$  angle of attack), signalling a sudden

drop in the vortex-induced thrust. It may be inferred that the chord dimension of LEVF III, while adequate within the  $C_L$  range of interest, was not sufficient to hold the vortex on the flap at higher angles of attack. The consequent migration of the vortex on to the wing then shows up in the lift and pitching-moment characteristics, already noted in figures 13 and 18 respectively.

Since leading-edge suction in potential flow is proportional to  $\sin^2 \alpha$ , the  $C_A$  data have been re-plotted in this relationship in fig. 20. The early leading-edge separation on the basic wing (around  $\alpha = 5^\circ$ ) causes the initial linear portion of the data to be compressed into a very small region on this plot. On the other hand, the LEVF data are notably linear over a substantial angle-of-attack range. From these data, an effective thrust coefficient  $C_T$  may be derived as follows:

$$C_T = - (C_A - C_{A_{\alpha=0}})$$

where  $C_{A_{\alpha=0}}$  was obtained by linear extrapolation to zero angle of attack, as shown in fig. 20. A thrust parameter ( $C_T \cos \alpha / C_N \sin \alpha$ ) may then be obtained (ref. 3) which relates the effective thrust component in the free-stream direction to the drag component from the normal force, where both  $C_T$  and  $C_N$  are derived from experiment as a function of angle of attack.

The thrust parameter is related to the lift-dependent drag coefficient as follows:

$$\begin{aligned} C_{D_L} &= C_N \sin \alpha - C_T \cos \alpha \\ &= C_L \tan \alpha (1 - C_T \cos \alpha / C_N \sin \alpha) \quad --- \end{aligned} \quad (1)$$

For zero leading-edge suction ( $C_T = 0$ ), eqn. (1) gives the familiar expression for lift-dependent drag

$$C_{D_L} = C_L \tan \alpha$$

whereas with full leading-edge suction, when  $C_{D_L} = C_L^2/\pi A$ , we get

$$(C_T \cos \alpha / C_N \sin \alpha)_{\max} = 1 - (C_L / \tan \alpha \cdot \pi \cdot A) \quad (2)$$

The thrust parameter is plotted versus angle of attack for the basic wing and the three LEVF configurations in fig. 21. Note that the flap-area effect does not appear in this presentation. The rapid decline of basic wing leading-edge suction due to early onset of separation is evident in fig. 21, whereas the vortex-flaps maintain a significant thrust level over the angle of attack range. The relative effectiveness of the different LEVF geometries is also well exhibited in this presentation, including the advantage of the extended flap configuration at the highest angles of attack.

Translating the effective thrust data to lift-dependent drag using eqn. 1 at  $10^\circ$  angle of attack, as an example, we get

$$\begin{aligned} C_{D_L} &= .053 \text{ for basic wing, and} \\ &= .035 \text{ for LEVF III} \end{aligned}$$

Thus, a 34-percent lift-dependent drag reduction is obtained by the use of LEVF III. Or, relative to the sharp leading edge basic wing for which  $C_{D_L} = C_L \tan \alpha = .06$ , the corresponding drag reduction is 41-percent.

#### CONCLUDING REMARKS

A preliminary subsonic wind-tunnel evaluation has been conducted of the leading edge vortex-flap (LEVF) concept of a  $74^\circ$  delta wing research model. The emphasis was on reducing the lift-dependent drag in the range of lift coefficient 0.4 to 0.6 appropriate to take-off, climb and landing phases. Of the various LEVF geometries investigated, the most promising was an inversely-tapered flap starting at 25-percent of the leading-edge length from the apex, having 15-percent of the wing area, a mean chord normal to the hinge-line equal to about 5-percent of wing mean aerodynamic chord, set at  $30^\circ$  deflection.

With this vortex-flap, drag reductions exceeding 30-percent relative to the blunt leading-edge basic wing (or 40-percent relative to sharp leading-edge wing) were indicated in the  $C_L$  range of interest. No adverse effects in the longitudinal stability characteristics by the use of vortex-flaps were noted.

The results of this exploratory investigation have established that vortex-flaps of a practical size can produce attractive performance improvements on highly swept, supersonic cruise type planforms for subsonic phases of flight. Continuation of the vortex-flap development for application to realistic aircraft configurations, taking into account practical design constraints, appear worth-while.

#### REFERENCES

1. Coe, Paul L., Jr. and Graham, A. B.; Results of Recent NASA Research on Low-Speed Aerodynamic Characteristics of Supersonic Cruise Aircraft. NASA CP-001, pp. 123-136. 1976.
2. Davenport, Edwin E. and Huffman, Jarrett K.; Experimental and Analytical Investigation of Subsonic Longitudinal and Lateral Characteristics of Slender Sharp-Edge 74 deg. Swept Wings. NASA TN D-6344, 1971.
3. Carlson, Harry W. and Mack, Robert J.; Estimation of Leading-Edge Thrust for Supersonic Wings of Arbitrary Planform. NASA TP 1270, 1978.

APPENDIX

WIND TUNNEL TEST SCHEDULES

Test # 54

Run no.	LEVF config.	$\delta_L$ (deg)	$d_{H.L.}$ (cm)	$\delta_T$ (deg)
3	I	30	1.27	
4			2.54	(TEF off)
5			3.81	
6		45	0	
7			1.27	
8			2.54	
9	(25% cut off)	30	1.27	
10	(50% cut off)		1.27	
11	(75% cut off)			
12	(LEVF off)			

Test # 58

1	I	45	1.27	30
2			2.54	(TEF off)
3				30
4				30
5				(TEF off)
6				(TEF off)
7				30
8				20
9				10
10				0
11				0
12				30
13	(void)			
14		30		30
15				0
16				20
17				10
18	(LEVF off)			10
19				20
20				0
21				30
22	III	30	1.27	30
23	III		1.27	0
24	IV		0	0
25	IV			47
26	IV			30



## NASA Langley

## 7 X 10 HIGH SPEED TUNNEL

54 RUN 3

MACH	Q	ALPHA PA	CL DEG	CD	CMS	CRMS	CYMS	CYS	L/D
.200	2777.5	-.08	-.0566	.0210	-.0076	-.0003	.0006	.0004	-2.69
.200	2764.6	-1.96	-.1354	.0307	-.0047	-.0004	.0004	-.0007	-4.41
.200	2784.1	-.08	-.0579	.0208	-.0078	-.0003	.0006	-.0003	-2.78
.201	2790.4	1.83	.0183	.0158	-.0121	.0001	.0006	.0003	1.16
.201	2795.0	3.79	.0939	.0161	-.0183	.0001	-.0000	.0004	5.84
.201	2796.9	5.64	.1586	.0216	-.0223	.0000	.0002	.0006	7.35
.200	2780.4	7.65	.2242	.0290	-.0239	-.0001	-.0002	.0017	7.74
.200	2778.9	9.63	.2837	.0373	-.0242	-.0003	.0003	.0014	7.61
.200	2769.1	11.58	.3525	.0495	-.0258	-.0004	.0006	.0006	7.12
.199	2753.9	13.61	.4403	.0700	-.0342	-.0001	.0000	.0002	6.29
.200	2773.9	15.68	.5409	.0996	-.0467	.0001	-.0000	-.0005	5.43
.200	2771.1	17.73	.6499	.1407	-.0551	.0009	.0003	-.0030	4.62
.200	2763.1	19.77	.7569	.1912	-.0633	.0011	.0005	-.0051	3.96
.200	2778.4	21.80	.8677	.2531	-.0701	.0022	.0014	-.0100	3.43
.200	2775.1	24.11	1.0104	.3416	-.0803	.0035	.0015	-.0161	2.96
.200	2771.5	-.10	-.0579	.0210	-.0073	-.0004	.0005	-.0001	-2.76

54 RUN 4

MACH	Q	ALPHA PA	CL DEG	CD	CMS	CRMS	CYMS	CYS	L/D
.200	2777.4	-.07	-.0525	.0214	-.0043	-.0006	.0001	.0009	-2.45
.201	2788.3	-1.94	-.1271	.0310	.0006	-.0007	-.0002	.0005	-4.10
.201	2794.0	-.07	-.0551	.0216	-.0041	-.0006	-.0001	.0008	-2.55
.201	2795.7	1.83	.0178	.0167	-.0104	-.0001	-.0002	.0011	1.06
.201	2787.0	3.78	.0907	.0178	-.0179	-.0002	-.0001	.0005	5.11
.201	2793.7	5.66	.1580	.0236	-.0245	-.0003	.0002	.0009	6.69
.200	2767.4	7.66	.2245	.0329	-.0296	-.0002	-.0003	.0018	6.82
.200	2777.4	9.57	.2842	.0431	-.0329	.0001	-.0002	.0009	6.59
.200	2763.1	11.56	.3466	.0554	-.0372	-.0001	-.0002	.0004	6.26
.200	2760.6	13.57	.4155	.0719	-.0444	.0000	-.0005	.0009	5.78
.199	2752.7	15.56	.5018	.0976	-.0592	-.0003	-.0002	.0012	5.14
.200	2770.7	17.67	.6023	.1348	-.0761	.0000	.0003	-.0002	4.47
.201	2782.2	19.64	.6902	.1745	-.0852	.0006	.0011	-.0026	3.96
.200	2775.6	21.65	.7781	.2209	-.0947	.0006	.0008	-.0028	3.52
.200	2780.5	23.92	.8915	.2866	-.1117	.0006	-.0001	-.0009	3.11
.201	2781.1	-.10	-.0542	.0214	-.0041	-.0005	-.0000	.0010	-2.53

54 RUN 5

MACH	Q	ALPHA PA	CL DEG	CD	CMS	CRMS	CYMS	CYS	L/D
.201	2797.9	-.05	-.0400	.0213	-.0021	-.0002	.0004	.0008	-1.88
.200	2791.4	-1.90	-.1053	.0299	.0036	-.0003	.0003	.0010	-3.52
.201	2797.6	-.06	-.0414	.0216	-.0022	-.0002	.0003	.0006	-1.92
.201	2807.2	1.87	.0255	.0176	-.0097	-.0000	.0001	.0009	1.45
.201	2800.6	3.79	.0971	.0194	-.0182	.0003	.0003	.0006	5.00
.201	2809.4	5.67	.1626	.0253	-.0261	.0001	.0007	.0002	6.42
.200	2795.8	7.67	.2311	.0366	-.0339	.0004	.0006	.0001	6.31
.200	2791.3	9.58	.2956	.0504	-.0404	.0007	.0006	-.0006	5.87
.200	2779.8	11.58	.3679	.0691	-.0479	.0008	.0003	.0000	5.32
.200	2777.3	13.58	.4342	.0902	-.0544	.0008	.0003	-.0013	4.81
.200	2773.4	15.60	.5041	.1149	-.0624	.0012	.0001	-.0015	4.39
.200	2785.6	17.63	.5803	.1467	-.0747	.0009	-.0004	-.0008	3.96
.201	2804.9	19.55	.6678	.1869	-.0926	.0005	-.0003	-.0007	3.57
.200	2787.6	21.61	.7565	.2339	-.1054	.0018	-.0011	.0008	3.23
.201	2806.4	23.68	.8455	.2897	-.1187	.0011	-.0015	.0019	2.92
.200	2787.3	-.10	-.0435	.0219	-.0022	-.0001	.0003	.0003	-1.99

## NASA Langley

## 7 X 10 HIGH SPEED TUNNEL

54 RUN 6

MACH	Q	ALPHA	CL	CD	CMS	CRMS	CYMS	CYS	L/D
	PA	DEG							
.201	2798.0	-.12	-.0717	.0279	-.0205	.0001	.0003	.0004	-2.57
.200	2785.1	-1.96	-.1512	.0396	-.0226	-.0001	.0001	.0006	-3.81
.201	2801.2	-.10	-.0714	.0282	-.0209	.0001	.0002	.0006	-2.54
.201	2810.7	1.86	.0088	.0205	-.0184	.0001	.0001	.0005	.43
.201	2793.8	3.80	.0839	.0182	-.0186	.0005	.0000	.0003	4.62
.201	2804.2	.5.71	.1479	.0204	-.0160	.0006	.0001	.0003	7.27
.200	2777.1	7.73	.2177	.0274	-.0173	.0004	-.0003	.0007	7.95
.200	2782.1	9.65	.2888	.0380	-.0155	.0004	.0001	.0005	7.60
.201	2793.7	11.69	.3676	.0529	-.0136	.0001	.0003	.0008	6.95
.200	2776.7	13.73	.4534	.0731	-.0135	.0002	.0003	.0003	6.20
.200	2779.9	15.77	.5515	.1018	-.0154	.0005	.0004	-.0008	5.42
.200	2769.3	17.88	.6694	.1429	-.0189	.0011	.0009	-.0023	4.69
.200	2787.3	19.87	.7882	.1932	-.0219	.0012	.0002	-.0029	4.08
.200	2786.1	22.03	.9230	.2601	-.0214	.0012	.0000	-.0026	3.55
.199	2760.1	24.14	1.0444	.3352	-.0149	.0016	.0000	-.0036	3.12
.200	2780.3	-.08	-.0687	.0279	-.0203	.0002	.0002	-.0007	-2.46

54 RUN 7

MACH	Q	ALPHA	CL	CD	CMS	CRMS	CYMS	CYS	L/D
	PA	DEG							
.200	2778.9	-.10	-.0689	.0292	-.0104	.0002	.0000	.0000	-2.36
.200	2778.6	-1.95	-.1429	.0403	-.0063	-.0001	-.0002	.0003	-3.54
.200	2786.7	-.11	-.0699	.0289	-.0103	.0001	-.0002	.0005	-2.41
.201	2796.5	1.85	.0093	.0225	-.0156	.0001	-.0000	.0004	.41
.200	2780.1	3.79	.0856	.0220	-.0214	.0001	.0002	.0009	3.89
.200	2777.4	5.68	.1595	.0266	-.0275	-.0001	.0003	.0009	6.00
.200	2776.0	7.70	.2320	.0357	-.0335	-.0000	.0002	.0010	6.50
.201	2795.3	9.59	.2980	.0470	-.0359	-.0001	-.0004	.0014	6.34
.200	2784.6	11.65	.3599	.0590	-.0362	-.0001	-.0011	.0026	6.10
.200	2784.7	13.63	.4253	.0738	-.0377	-.0008	-.0011	.0024	5.76
.200	2786.1	15.63	.4979	.0939	-.0426	-.0000	-.0019	.0018	5.30
.200	2772.0	17.72	.5945	.1260	-.0579	-.0015	-.0011	.0034	4.72
.200	2784.7	19.64	.6973	.1663	-.0762	-.0024	-.0012	.0052	4.19
.201	2789.7	21.72	.8010	.2147	-.0900	-.0022	-.0022	.0077	3.73
.201	2789.0	23.77	.8951	.2684	-.0971	-.0035	-.0040	.0131	3.33
.200	2776.1	-.12	-.0660	.0289	-.0102	.0003	.0002	.0005	-2.28

54 RUN 8

MACH	Q	ALPHA	CL	CD	CMS	CRMS	CYMS	CYS	L/D
	PA	DEG							
.201	2786.5	-.09	-.0647	.0292	-.0071	-.0001	-.0003	-.0002	-2.21
.200	2772.6	-1.93	-.1308	.0395	-.0021	.0000	-.0004	-.0002	-3.31
.201	2787.8	-.09	-.0637	.0292	-.0071	.0002	-.0003	-.0001	-2.18
.201	2784.2	1.83	.0086	.0231	-.0138	.0001	-.0005	-.0002	.37
.201	2783.9	3.76	.0826	.0231	-.0211	.0003	-.0000	.0006	3.58
.201	2778.9	5.66	.1543	.0277	-.0284	.0002	.0000	.0001	5.57
.200	2771.9	7.67	.2286	.0377	-.0357	.0001	.0002	.0001	6.06
.200	2767.7	9.57	.2969	.0517	-.0413	.0007	-.0000	-.0015	5.75
.200	2751.6	11.58	.3667	.0685	-.0455	.0010	-.0008	-.0016	5.35
.200	2765.2	13.59	.4352	.0883	-.0507	.0013	-.0016	-.0016	4.93
.200	2768.8	15.58	.5035	.1098	-.0563	.0009	-.0024	.0006	4.59
.200	2758.0	17.64	.5736	.1361	-.0637	.0004	-.0030	.0010	4.21
.200	2757.6	19.54	.6494	.1677	-.0763	-.0008	-.0033	.0038	3.87
.201	2776.2	21.61	.7525	.2161	-.0978	-.0009	-.0028	.0042	3.48
.200	2762.5	23.73	.8539	.2731	-.1170	-.0017	-.0015	.0035	3.13
.201	2779.4	-.11	-.0638	.0293	-.0072	.0001	-.0004	-.0010	-2.18

## NASA Langley

## 7 X 10 HIGH SPEED TUNNEL

54 RUN 9

MACH	Q	ALPHA PA	CL	CD	CMS	CRMS	CYMS	CYS	L/D
		DEG							
.200	2765.5	-.06	-.0510	.0188	.0005	-.0001	.0004	-.0005	-2.72
.200	2764.2	-1.91	-.1233	.0274	.0063	-.0001	.0006	-.0005	-4.50
.201	2777.1	-.06	-.0499	.0189	.0005	-.0001	.0004	-.0005	-2.65
.201	2776.8	1.85	.0259	.0141	-.0067	.0002	.0004	-.0006	1.83
.201	2781.9	3.78	.1001	.0144	-.0150	.0002	.0001	-.0008	6.96
.200	2763.5	5.68	.1642	.0206	-.0213	.0001	.0001	-.0011	7.96
.200	2756.8	7.69	.2323	.0289	-.0239	-.0000	-.0001	.0006	8.03
.200	2744.5	9.59	.2953	.0385	-.0254	-.0000	.0001	-.0012	7.67
.200	2756.8	11.64	.3691	.0540	-.0292	.0006	-.0006	-.0031	6.84
.200	2753.8	13.66	.4570	.0773	-.0384	.0008	-.0012	-.0028	5.91
.200	2754.1	15.68	.5614	.1108	-.0521	.0014	-.0018	-.0048	5.07
.201	2778.0	17.76	.6668	.1546	-.0620	.0024	-.0031	-.0066	4.31
.200	2770.0	19.72	.7626	.2042	-.0674	.0041	-.0028	-.0130	3.73
.200	2761.9	21.86	.9087	.2901	-.0816	.0019	.0052	-.0366	3.13
.200	2758.4	24.05	1.0616	.3899	-.0928	.0029	.0009	-.0226	2.72
.201	2772.8	-.07	-.0473	.0186	.0005	.0000	.0005	-.0020	-2.55

54 RUN 10

MACH	Q	ALPHA PA	CL	CD	CMS	CRMS	CYMS	CYS	L/D
		DEG							
.201	2773.8	-.03	-.0396	.0157	.0061	-.0007	-.0003	.0004	-2.53
.200	2759.7	-1.90	-.1075	.0229	.0154	-.0006	-.0004	.0010	-4.69
.201	2776.9	-.03	-.0406	.0157	.0063	-.0006	-.0004	.0010	-2.58
.201	2780.5	1.87	.0290	.0123	-.0034	-.0004	-.0004	.0009	2.37
.201	2776.6	3.79	.0987	.0135	-.0134	-.0003	-.0002	.0002	7.33
.200	2770.8	5.69	.1665	.0206	-.0227	.0002	-.0002	-.0001	8.08
.200	2760.0	7.69	.2334	.0302	-.0271	.0005	-.0005	.0015	7.72
.200	2767.2	9.58	.3001	.0428	-.0312	.0004	.0001	-.0003	7.01
.200	2757.6	11.62	.3766	.0615	-.0357	.0012	-.0006	-.0035	6.13
.200	2757.9	13.63	.4536	.0844	-.0411	.0017	.0002	-.0085	5.38
.200	2756.8	15.66	.5419	.1156	-.0505	.0024	-.0010	-.0091	4.69
.200	2765.4	17.74	.6402	.1570	-.0606	.0033	-.0020	-.0082	4.08
.200	2765.0	19.69	.7376	.2073	-.0688	.0041	.0002	-.0094	3.56
.200	2770.5	21.82	.8765	.2935	-.0892	.0031	-.0007	-.0083	2.99
.200	2751.3	24.00	1.0727	.4165	-.1260	.0062	-.0079	.0027	2.58
.200	2760.0	-.07	-.0411	.0157	.0063	-.0007	-.0003	.0005	-2.61

54 RUN 11

MACH	Q	ALPHA PA	CL	CD	CMS	CRMS	CYMS	CYS	L/D
		DEG							
.200	2796.7	-.02	-.0262	.0133	.0106	.0001	.0002	-.0001	-1.98
.200	2793.3	-1.86	-.0894	.0183	.0225	-.0001	.0000	.0005	-4.89
.201	2813.2	-.01	-.0267	.0130	.0106	-.0002	.0000	.0002	-2.05
.201	2810.1	1.88	.0357	.0110	-.0012	.0002	-.0000	-.0003	3.25
.200	2787.5	3.78	.0987	.0127	-.0127	.0005	-.0000	-.0004	7.75
.200	2793.9	5.69	.1716	.0213	-.0258	.0007	.0002	-.0001	8.04
.200	2784.4	7.67	.2425	.0332	-.0364	.0007	.0008	-.0010	7.30
.200	2789.0	9.57	.3163	.0497	-.0450	.0004	.0001	-.0007	6.37
.200	2781.6	11.61	.4000	.0736	-.0540	.0012	-.0002	-.0046	5.43
.199	2767.7	13.64	.4895	.1050	-.0637	.0018	-.0009	-.0057	4.66
.200	2797.6	15.65	.5783	.1415	-.0745	.0019	-.0015	-.0078	4.09
.199	2770.7	17.74	.6777	.1893	-.0872	.0016	-.0021	-.0092	3.58
.201	2811.5	19.68	.7748	.2436	-.0986	.0029	-.0033	-.0072	3.18
.200	2787.4	21.77	.8821	.3136	-.1131	.0040	-.0028	-.0070	2.81
.200	2779.5	23.88	.9923	.3979	-.1327	.0049	-.0058	-.0052	2.49
.200	2789.7	-.03	-.0277	.0128	.0107	.0001	.0002	-.0006	-2.16

## NASA Langley

## 7 X 10 HIGH SPEED TUNNEL

54 RUN 12

MACH	Q	ALPHA	CL	CD	CMS	CRMS	CYMS	CYS	L/D
	PA	DEG							
.201	2803.4	.01	.0081	.0093	-.0016	-.0000	-.0001	.0006	.88
.200	2786.8	-1.83	-.0341	.0097	.0036	.0004	.0000	.0004	-3.52
.200	2795.4	.00	.0082	.0091	-.0017	-.0001	-.0001	.0004	.91
.201	2803.4	1.88	.0540	.0098	-.0078	.0001	-.0001	.0001	5.53
.201	2811.0	3.79	.1037	.0125	-.0150	.0004	-.0003	.0002	8.27
.201	2816.9	5.68	.1655	.0211	-.0258	.0001	.0001	-.0000	7.84
.200	2797.5	7.67	.2360	.0347	-.0355	.0001	.0007	.0002	6.81
.200	2788.1	9.57	.3029	.0516	-.0444	.0002	.0014	-.0017	5.87
.199	2773.6	11.60	.3840	.0771	-.0560	.0014	.0003	-.0031	4.98
.200	2779.5	13.62	.4670	.1095	-.0657	.0025	-.0013	-.0041	4.27
.199	2774.2	15.63	.5548	.1487	-.0769	.0031	-.0023	-.0065	3.73
.200	2797.8	17.70	.6410	.1945	-.0882	.0035	-.0028	-.0087	3.29
.200	2793.1	19.64	.7337	.2493	-.0992	.0038	-.0034	-.0066	2.94
.200	2791.8	21.71	.8283	.3140	-.1111	.0039	-.0039	-.0051	2.64
.200	2801.6	23.82	.9286	.3892	-.1237	.0036	-.0049	-.0045	2.39
.201	2816.1	-.03	.0088	.0094	-.0018	.0000	-.0002	-.0001	.94

( End of Test 54 )

58 RUN 1

MACH	Q	ALPHA	CL	CD	CMS	CRMS	CYMS	CYS	L/D
	PA	DEG							
.201	2790.5	-.04	.1530	.0412	-.1185	.0012	.0003	-.0004	3.72
.200	2779.1	-1.86	.0816	.0440	-.1136	.0012	.0007	-.0008	1.85
.200	2784.6	-.05	.1530	.0414	-.1190	.0014	.0005	-.0008	3.69
.201	2799.7	1.89	.2250	.0426	-.1236	.0009	-.0001	-.0003	5.29
.200	2786.5	3.80	.2987	.0496	-.1316	.0011	-.0003	-.0002	6.02
.200	2766.4	5.69	.3816	.0652	-.1460	.0014	-.0004	.0006	5.85
.200	2781.5	7.69	.4703	.0860	-.1622	.0010	-.0005	.0015	5.47
.201	2793.6	9.60	.5459	.1058	-.1684	-.0002	-.0007	.0030	5.16
.199	2750.6	11.61	.6182	.1276	-.1704	.0004	-.0005	.0001	4.85
.200	2769.8	13.69	.7134	.1592	-.1803	.0009	-.0016	-.0037	4.48
.199	2759.2	15.66	.8011	.1948	-.1891	.0010	-.0029	-.0046	4.11
.198	2727.7	17.78	.9110	.2452	-.2051	.0015	-.0043	-.0036	3.72
.201	2796.0	17.78	.9127	.2453	-.2050	.0027	-.0045	-.0057	3.72
.201	2790.3	19.83	1.0287	.3052	-.2217	.0031	-.0062	-.0059	3.37
.201	2807.0	21.86	1.1431	.3778	-.2373	.0041	-.0061	-.0110	3.03
.200	2783.1	23.79	1.2603	.4636	-.2533	.0033	-.0037	-.0158	2.72
.201	2806.6	-.07	.1512	.0413	-.1185	.0012	.0003	-.0006	3.66

58 RUN 2

MACH	Q	ALPHA	CL	CD	CMS	CRMS	CYMS	CYS	L/D
	PA	DEG							
.201	2791.8	-.07	-.0638	.0233	-.0004	.0004	.0006	-.0005	-2.73
.201	2790.5	-1.91	-.1385	.0331	.0046	.0003	.0006	-.0007	-4.19
.201	2800.8	-.08	-.0646	.0229	-.0004	.0002	.0005	-.0013	-2.83
.201	2797.2	1.85	.0116	.0173	-.0061	.0006	.0003	-.0016	.67
.200	2785.2	3.77	.0857	.0167	-.0130	.0003	-.0000	-.0006	5.13
.200	2787.0	5.66	.1644	.0216	-.0217	.0005	-.0000	-.0005	7.62
.200	2781.0	7.68	.2375	.0312	-.0284	.0000	.0001	.0007	7.60
.200	2783.5	9.54	.3077	.0429	-.0324	-.0003	-.0001	.0009	7.18
.200	2785.9	11.58	.3805	.0574	-.0335	-.0004	-.0004	.0003	6.63
.200	2767.8	13.61	.4604	.0777	-.0372	.0007	-.0012	-.0035	5.93
.201	2794.6	15.63	.5509	.1058	-.0447	.0013	-.0026	-.0052	5.21
.200	2782.2	17.72	.6518	.1443	-.0556	.0026	-.0034	-.0060	4.52
.200	2781.6	19.68	.7441	.1864	-.0626	.0034	-.0049	-.0087	3.99
.200	2781.5	21.78	.8466	.2444	-.0696	.0030	-.0051	-.0110	3.46
.201	2792.4	23.72	.9495	.3119	-.0763	.0045	-.0044	-.0182	3.04
.201	2796.4	-.09	-.0626	.0231	-.0002	.0004	.0005	-.0009	-2.72

## NASA Langley

## 7 X 10 HIGH SPEED TUNNEL

58 RUN 3

MACH	Q	ALPHA PA DEG	CL	CD	CMS	CRMS	CYMS	CYS	L/D
.200	2778.7	-.04	.1550	.0395	-.1195	.0005	.0003	-.0003	3.93
.200	2776.9	-1.87	.0812	.0416	-.1137	.0002	.0005	-.0010	1.95
.201	2799.4	-.05	.1558	.0390	-.1193	.0006	.0001	-.0008	3.99
.200	2781.2	1.85	.2287	.0409	-.1258	.0008	.0002	-.0012	5.59
.200	2784.6	3.79	.3056	.0480	-.1347	.0008	-.0004	-.0008	6.37
.200	2768.8	5.67	.3854	.0624	-.1473	.0011	-.0001	-.0002	6.17
.200	2785.4	7.67	.4710	.0818	-.1617	.0010	.0001	-.0006	5.76
.200	2783.5	9.57	.5468	.1010	-.1672	.0001	.0002	-.0002	5.42
.199	2760.4	11.62	.6232	.1247	-.1711	.0002	-.0003	-.0004	5.00
.200	2776.6	13.65	.7099	.1542	-.1778	.0004	-.0018	-.0031	4.60
.200	2783.5	15.70	.7996	.1906	-.1872	.0014	-.0025	-.0058	4.19
.200	2787.1	17.76	.9133	.2409	-.2040	.0023	-.0039	-.0061	3.79
.201	2791.3	19.73	1.0237	.2988	-.2208	.0023	-.0054	-.0070	3.43
.200	2786.8	21.86	1.1447	.3753	-.2364	.0044	-.0050	-.0135	3.05
.200	2765.4	23.70	1.2573	.4574	-.2524	.0050	-.0025	-.0196	2.75
.200	2778.7	-.06	.1547	.0394	-.1193	.0003	.0004	-.0007	3.92

58 RUN 4

MACH	Q	ALPHA PA DEG	CL	CD	CMS	CRMS	CYMS	CYS	L/D
.201	2809.5	-.03	.1630	.0409	-.1227	.0007	-.0003	-.0013	3.98
.200	2807.4	-1.82	.0919	.0427	-.1154	.0001	-.0007	.0001	2.16
.201	2813.5	-.03	.1601	.0408	-.1221	.0005	-.0004	-.0006	3.92
.200	2807.6	1.91	.2375	.0433	-.1317	.0001	.0001	-.0012	5.48
.201	2809.6	3.82	.3105	.0521	-.1403	.0008	-.0001	-.0011	5.96
.200	2801.6	5.73	.3849	.0658	-.1512	.0010	-.0002	-.0003	5.85
.200	2787.7	7.71	.4681	.0855	-.1651	.0007	-.0002	-.0002	5.47
.201	2811.5	9.61	.5364	.1051	-.1708	.0007	-.0005	-.0002	5.10
.200	2787.2	11.66	.6079	.1284	-.1752	.0011	-.0011	-.0007	4.73
.199	2778.5	13.62	.6790	.1540	-.1813	.0018	-.0024	-.0033	4.41
.200	2805.8	15.65	.7612	.1881	-.1930	.0019	-.0026	-.0054	4.05
.199	2765.2	17.72	.8537	.2306	-.2078	.0024	-.0061	-.0030	3.70
.200	2783.6	19.73	.9524	.2813	-.2261	.0031	-.0073	-.0059	3.39
.201	2834.3	21.83	1.0736	.3518	-.2486	.0028	-.0075	-.0075	3.05
.200	2797.8	23.72	1.1888	.4279	-.2679	.0031	-.0088	-.0105	2.78
.200	2795.6	-.04	.1596	.0408	-.1224	.0004	-.0004	-.0012	3.91

58 RUN 5

MACH	Q	ALPHA PA DEG	CL	CD	CMS	CRMS	CYMS	CYS	L/D
.200	2799.1	-.07	-.0583	.0230	-.0011	.0005	-.0001	-.0016	-2.53
.200	2802.2	-1.87	-.1288	.0324	.0040	.0004	-.0003	-.0011	-3.97
.201	2819.3	-.05	-.0592	.0227	-.0011	.0002	-.0004	-.0014	-2.60
.201	2820.6	1.96	.0186	.0179	-.0089	.0005	-.0002	-.0009	1.04
.201	2814.9	3.79	.0907	.0184	-.0162	.0004	.0000	-.0003	4.93
.201	2809.9	5.77	.1654	.0231	-.0247	-.0001	.0000	-.0004	7.16
.200	2801.1	7.70	.2354	.0332	-.0314	.0002	.0002	-.0002	7.08
.200	2787.7	9.57	.3009	.0450	-.0354	-.0001	.0000	-.0011	6.68
.201	2819.1	11.66	.3682	.0591	-.0360	.0006	-.0007	-.0010	6.23
.200	2795.5	13.61	.4311	.0750	-.0376	.0004	-.0016	-.0014	5.74
.201	2808.1	15.63	.5072	.0990	-.0433	.0009	-.0029	-.0038	5.13
.200	2803.9	17.70	.5918	.1307	-.0529	.0002	-.0057	.0001	4.53
.201	2808.0	19.64	.6856	.1709	-.0663	.0010	-.0064	-.0022	4.01
.198	2747.3	21.75	.7967	.2264	-.0831	.0006	-.0075	-.0051	3.52
.201	2807.6	23.64	.8851	.2815	-.0941	.0013	-.0098	-.0081	3.14
.201	2807.7	-.07	-.0602	.0232	-.0012	.0005	-.0002	-.0011	-2.60

## NASA Langley

## 7 X 10 HIGH SPEED TUNNEL

58 RUN 6

MACH	Q PA	ALPHA DEG	CL	CD	CMS	CRMS	CYMS	CYS	L/D
.200	2797.9	-.07	-.0559	.0221	.0007	.0003	.0001	.0002	-2.53
.201	2807.0	-1.90	-.1231	.0304	.0068	.0004	.0002	-.0005	-4.04
.201	2824.5	-.07	-.0537	.0216	.0004	.0003	.0002	-.0004	-2.49
.200	2801.1	1.87	.0206	.0171	-.0071	.0005	.0003	-.0001	1.21
.201	2811.4	3.79	.0909	.0176	-.0152	.0006	.0003	-.0006	5.15
.200	2791.8	5.70	.1642	.0229	-.0238	.0002	.0005	-.0002	7.18
.199	2777.6	7.66	.2336	.0327	-.0313	.0004	.0005	.0005	7.14
.201	2816.3	9.55	.3018	.0451	-.0360	.0003	.0003	.0010	6.69
.200	2797.9	11.59	.3680	.0593	-.0376	.0005	-.0003	.0007	6.21
.200	2786.8	13.58	.4330	.0764	-.0397	.0008	-.0003	-.0023	5.67
.201	2807.7	15.61	.5114	.0998	-.0453	.0012	-.0016	-.0045	5.12
.201	2813.1	17.67	.6022	.1352	-.0567	-.0002	-.0031	-.0008	4.46
.200	2789.2	19.62	.6916	.1745	-.0682	.0014	-.0017	-.0055	3.96
.201	2816.7	21.79	.8026	.2329	-.0834	.0020	-.0017	-.0070	3.45
.200	2785.5	23.60	.8799	.2837	-.0918	.0005	-.0038	-.0049	3.10
.200	2786.8	-.08	-.0551	.0220	.0008	.0007	.0005	-.0006	-2.51

58 RUN 7

MACH	Q PA	ALPHA DEG	CL	CD	CMS	CRMS	CYMS	CYS	L/D
.200	2793.9	-.03	.1602	.0395	-.1180	-.0000	-.0002	-.0000	4.06
.200	2799.8	-1.84	.0922	.0407	-.1118	.0005	-.0002	-.0008	2.26
.201	2808.8	-.02	.1583	.0392	-.1178	-.0002	-.0003	.0003	4.03
.200	2801.8	1.91	.2305	.0421	-.1268	.0000	-.0001	-.0001	5.47
.201	2808.9	3.84	.3077	.0516	-.1368	.0008	-.0002	-.0000	5.96
.200	2795.7	5.74	.3856	.0655	-.1495	.0010	.0000	.0002	5.89
.200	2799.6	7.74	.4706	.0861	-.1657	.0008	.0001	-.0006	5.47
.200	2798.7	9.65	.5439	.1069	-.1734	.0010	-.0002	-.0005	5.09
.200	2783.5	11.66	.6125	.1293	-.1784	.0015	-.0007	-.0021	4.74
.200	2779.6	13.65	.6865	.1567	-.1854	.0012	-.0012	-.0022	4.38
.200	2784.5	15.70	.7600	.1868	-.1910	.0014	-.0019	-.0044	4.07
.201	2820.2	17.74	.8530	.2299	-.2049	.0016	-.0029	-.0041	3.71
.200	2800.0	19.68	.9483	.2805	-.2205	.0022	-.0025	-.0072	3.38
.201	2827.7	21.80	1.0616	.3488	-.2410	.0009	-.0031	-.0074	3.04
.200	2801.2	23.66	1.1549	.4156	-.2570	-.0001	-.0055	-.0035	2.78
.200	2794.8	-.02	.1595	.0389	-.1180	.0004	-.0002	-.0012	4.10

58 RUN 8

MACH	Q PA	ALPHA DEG	CL	CD	CMS	CRMS	CYMS	CYS	L/D
.200	2802.2	-.05	.0970	.0289	-.0843	.0004	-.0002	-.0007	3.36
.200	2794.7	-1.84	.0304	.0327	-.0788	.0007	-.0002	-.0009	.93
.201	2809.5	-.04	.0955	.0287	-.0842	.0004	-.0002	-.0009	3.33
.200	2798.4	1.89	.1662	.0291	-.0912	.0004	-.0000	-.0001	5.71
.200	2793.1	3.84	.2401	.0355	-.0990	.0004	-.0001	.0000	6.76
.200	2790.1	5.71	.3122	.0459	-.1094	.0010	.0003	-.0006	6.80
.200	2784.5	7.70	.3943	.0631	-.1225	.0006	.0001	-.0001	6.25
.201	2820.1	9.68	.4665	.0813	-.1297	.0006	-.0001	.0000	5.74
.201	2811.4	11.69	.5338	.1010	-.1327	.0013	-.0008	-.0002	5.28
.199	2778.0	13.62	.6082	.1248	-.1392	.0012	-.0010	-.0008	4.87
.201	2810.4	15.69	.6800	.1536	-.1459	.0020	-.0019	-.0044	4.43
.200	2787.0	17.77	.7779	.1954	-.1607	.0003	-.0031	-.0019	3.98
.200	2785.6	19.66	.8741	.2433	-.1768	.0019	-.0030	-.0067	3.59
.200	2796.3	21.76	.9872	.3082	-.1962	.0017	-.0030	-.0076	3.20
.202	2837.5	23.64	1.0937	.3771	-.2141	-.0003	-.0053	-.0034	2.90
.200	2788.3	-.04	.0967	.0289	-.0841	.0006	-.0001	-.0004	3.34

## NASA Langley

## 7 X 10 HIGH SPEED TUNNEL

58 RUN 9

MACH	Q	ALPHA PA	CL	CD	CMS	CRMS	CYMS	CYS	L/D
		DEG							
.201	2807.4	-.06	.0207	.0240	-.0421	.0004	.0002	-.0004	.86
.200	2802.8	-1.85	-.0475	.0300	-.0358	.0004	.0001	-.0007	-1.58
.200	2797.9	-.04	.0199	.0237	-.0421	.0003	.0001	-.0007	.84
.201	2814.2	1.89	.0918	.0216	-.0489	.0007	.0003	-.0010	4.24
.200	2800.1	3.82	.1627	.0247	-.0556	.0006	.0001	-.0001	6.58
.200	2786.0	5.74	.2337	.0323	-.0645	.0005	.0002	-.0002	7.23
.200	2781.0	7.68	.3127	.0461	-.0759	.0006	.0006	-.0006	6.78
.201	2804.9	9.65	.3872	.0619	-.0841	.0006	.0003	-.0008	6.25
.200	2797.4	11.62	.4569	.0795	-.0883	.0009	-.0006	.0002	5.75
.200	2789.8	13.61	.5318	.1012	-.0954	.0017	-.0006	-.0027	5.26
.200	2797.7	15.63	.6068	.1278	-.1026	.0013	-.0020	-.0050	4.75
.200	2787.0	17.71	.6995	.1657	-.1160	.0018	-.0027	-.0040	4.22
.200	2801.8	19.66	.8032	.2134	-.1319	.0017	-.0029	-.0060	3.76
.201	2804.4	21.77	.9231	.2786	-.1533	.0017	-.0023	-.0079	3.31
.200	2786.9	23.61	1.0129	.3379	-.1675	.0004	-.0042	-.0042	3.00
.201	2804.9	-.06	.0231	.0238	-.0423	.0005	.0001	-.0007	.97

58 RUN 11

MACH	Q	ALPHA PA	CL	CD	CMS	CRMS	CYMS	CYS	L/D
		DEG							
.200	2791.9	-.07	-.0392	.0228	-.0092	.0006	.0006	-.0009	-1.72
.201	2801.7	-1.86	-.1108	.0316	-.0033	.0006	.0008	-.0005	-3.51
.200	2787.7	-.04	-.0365	.0225	-.0089	.0004	.0006	-.0004	-1.63
.200	2794.0	1.88	.0360	.0183	-.0149	.0008	.0005	-.0004	1.96
.201	2807.4	3.79	.1100	.0189	-.0215	.0006	.0001	.0003	5.83
.201	2798.3	5.69	.1779	.0243	-.0278	.0007	.0001	.0004	7.32
.201	2797.2	7.69	.2570	.0351	-.0377	.0006	.0000	.0012	7.33
.200	2781.2	9.59	.3322	.0478	-.0451	.0003	-.0003	.0006	6.95
.200	2793.6	11.63	.4094	.0637	-.0504	.0004	-.0003	.0004	6.42
.200	2791.1	13.64	.4873	.0851	-.0559	.0003	-.0007	-.0000	5.73
.201	2799.4	15.66	.5696	.1114	-.0617	.0007	-.0015	-.0028	5.11
.200	2785.4	17.75	.6691	.1494	-.0734	.0006	-.0021	-.0041	4.48
.200	2793.2	19.75	.7795	.1992	-.0870	.0021	-.0006	-.0097	3.91
.201	2804.7	21.83	.9056	.2670	-.1051	.0028	-.0030	-.0121	3.39
.200	2793.2	23.74	1.0151	.3368	-.1205	.0014	-.0035	-.0102	3.01
.200	2784.4	-.07	-.0384	.0227	-.0090	.0006	.0006	-.0004	-1.69

58 RUN 10

MACH	Q	ALPHA PA	CL	CD	CMS	CRMS	CYMS	CYS	L/D
		DEG							
.200	2792.4	-.05	-.0302	.0224	-.0109	.0003	-.0001	-.0012	-1.35
.200	2784.2	-1.85	-.0993	.0304	-.0042	.0002	-.0000	-.0003	-3.26
.201	2807.6	-.03	-.0293	.0224	-.0109	.0002	-.0001	-.0009	-1.31
.201	2802.0	1.92	.0421	.0181	-.0176	.0002	-.0001	-.0009	2.33
.201	2808.5	3.80	.1085	.0202	-.0227	.0004	-.0001	.0003	5.38
.200	2793.9	5.69	.1797	.0256	-.0308	.0003	.0001	-.0001	7.03
.200	2778.7	7.70	.2591	.0375	-.0418	.0004	.0002	-.0019	6.91
.200	2781.0	9.64	.3334	.0520	-.0498	.0008	.0000	-.0014	6.41
.200	2789.3	11.62	.4008	.0669	-.0543	.0009	-.0007	-.0013	5.99
.201	2799.7	13.64	.4811	.0884	-.0614	.0013	-.0009	-.0034	5.44
.201	2812.1	15.67	.5534	.1127	-.0679	.0008	-.0014	-.0039	4.91
.200	2772.9	17.75	.6485	.1500	-.0818	.0003	-.0034	-.0010	4.32
.200	2786.7	19.67	.7406	.1912	-.0943	-.0002	-.0035	-.0022	3.87
.201	2819.1	21.79	.8640	.2557	-.1160	.0018	-.0020	-.0082	3.38
.200	2777.7	23.62	.9531	.3129	-.1288	.0003	-.0048	-.0061	3.05
.200	2784.1	-.05	-.0311	.0224	-.0105	.0003	-.0000	-.0015	-1.39

## NASA Langley

## 7 X 10 HIGH SPEED TUNNEL

58 RUN 12

MACH	Q PA	ALPHA DEG	CL	CD	CMS	CRMS	CYMS	CYS	L/D
.200	2786.4	-.04	.1637	.0397	-.1218	.0006	.0007	-.0009	4.12
.200	2793.1	-1.84	.0969	.0416	-.1167	.0007	.0009	-.0016	2.33
.201	2795.3	-.00	.1669	.0396	-.1219	.0007	.0007	-.0012	4.22
.201	2803.2	1.92	.2375	.0421	-.1284	.0009	.0005	-.0008	5.65
.200	2788.7	3.89	.3188	.0513	-.1398	.0007	-.0001	.0001	6.21
.201	2798.3	5.72	.3946	.0656	-.1518	.0012	.0002	-.0002	6.01
.200	2793.2	7.73	.4809	.0858	-.1664	.0007	.0001	.0005	5.60
.200	2793.2	9.66	.5581	.1056	-.1738	.0002	-.0003	.0001	5.29
.201	2804.1	11.66	.6283	.1282	-.1771	.0001	-.0005	-.0005	4.90
.201	2798.1	13.70	.7087	.1558	-.1823	.0004	-.0008	-.0017	4.55
.200	2782.3	15.70	.7851	.1879	-.1867	.0008	-.0017	-.0042	4.18
.201	2796.3	17.81	.8896	.2349	-.2000	.0010	-.0025	-.0057	3.79
.201	2803.9	19.78	1.0068	.2949	-.2180	.0025	-.0021	-.0109	3.41
.200	2774.3	21.92	1.1302	.3719	-.2365	.0023	-.0034	-.0127	3.04
.200	2784.6	23.80	1.2446	.4539	-.2538	.0002	-.0043	-.0105	2.74
.201	2802.0	-.04	.1660	.0394	-.1219	.0005	.0006	-.0012	4.22

58 RUN 14

MACH	Q PA	ALPHA DEG	CL	CD	CMS	CRMS	CYMS	CYS	L/D
.200	2793.9	-.01	.1708	.0340	-.1138	.0009	.0008	-.0023	5.03
.200	2799.6	-1.81	.1030	.0346	-.1085	.0009	.0009	-.0026	2.97
.201	2808.2	.01	.1748	.0337	-.1138	.0007	.0006	-.0028	5.19
.201	2807.9	1.94	.2471	.0374	-.1211	.0011	.0004	-.0022	6.61
.200	2796.6	3.88	.3207	.0473	-.1312	.0011	.0000	-.0015	6.78
.200	2787.7	5.74	.3983	.0613	-.1430	.0012	-.0003	-.0009	6.49
.200	2799.4	7.85	.4889	.0807	-.1525	.0006	-.0001	-.0015	6.05
.200	2801.5	9.66	.5559	.0993	-.1561	-.0003	.0000	-.0006	5.60
.200	2777.4	11.71	.6548	.1289	-.1640	-.0001	.0002	-.0018	5.08
.200	2789.7	13.91	.7664	.1710	-.1763	.0004	.0006	-.0043	4.48
.200	2787.1	15.82	.8864	.2234	-.1919	.0009	.0003	-.0080	3.97
.200	2800.4	17.96	1.0231	.2977	-.2118	.0008	-.0003	-.0088	3.44
.199	2759.7	19.96	1.1841	.3915	-.2386	-.0020	.0023	-.0166	3.02
.200	2783.1	22.18	1.3553	.5066	-.2544	.0021	-.0031	-.0143	2.68
.199	2768.8	24.08	1.4706	.6022	-.2614	-.0018	-.0056	-.0067	2.44
.201	2809.6	-.00	.1736	.0339	-.1136	.0012	.0011	-.0040	5.13

58 RUN 15

MACH	Q PA	ALPHA DEG	CL	CD	CMS	CRMS	CYMS	CYS	L/D
.201	2816.6	-.05	-.0257	.0176	-.0045	.0002	.0004	-.0006	-1.45
.200	2795.4	-1.83	-.1002	.0245	.0022	.0004	.0008	-.0011	-4.09
.201	2814.0	-.01	-.0235	.0175	-.0047	.0001	.0004	-.0001	-1.35
.201	2809.8	1.91	.0538	.0140	-.0127	.0001	.0001	-.0003	3.85
.201	2820.5	3.81	.1225	.0160	-.0197	.0001	.0001	.0006	7.64
.200	2802.6	5.72	.1894	.0221	-.0247	-.0001	-.0003	.0012	8.56
.201	2810.0	7.71	.2662	.0315	-.0307	-.0001	-.0000	.0004	8.46
.201	2823.5	9.63	.3436	.0452	-.0348	.0001	-.0001	.0008	7.60
.201	2805.9	11.67	.4336	.0662	-.0412	-.0008	.0001	.0005	6.56
.200	2789.3	13.74	.5371	.0977	-.0504	.0005	.0010	-.0020	5.50
.200	2787.8	15.77	.6547	.1415	-.0635	.0015	.0007	-.0079	4.63
.201	2816.2	17.89	.7819	.2012	-.0776	.0010	-.0000	-.0077	3.89
.201	2811.5	19.93	.9277	.2781	-.0963	-.0005	.0005	-.0110	3.34
.201	2811.1	22.07	1.0846	.3740	-.1091	.0002	-.0025	-.0107	2.90
.201	2813.8	24.02	1.2227	.4680	-.1208	-.0019	-.0052	-.0046	2.61
.201	2805.0	-.05	-.0265	.0175	-.0045	.0003	.0004	-.0009	-1.51

## NASA Langley

## 7 X 10 HIGH SPEED TUNNEL

58 RUN 16

MACH	Q	ALPHA	CL	CD	CMS	CRMS	CYMS	CYS	L/D
	PA	DEG							
.200	2804.4	-.02	.1004	.0236	-.0762	.0009	.0003	-.0016	4.26
.200	2794.0	-1.82	.0307	.0268	-.0710	.0006	.0005	-.0011	1.14
.201	2821.0	.02	.1026	.0235	-.0765	.0004	.0003	-.0010	4.36
.200	2801.3	1.93	.1776	.0246	-.0832	.0004	.0001	-.0004	7.22
.201	2807.9	3.84	.2438	.0307	-.0897	.0003	-.0002	.0001	7.93
.200	2797.9	5.71	.3159	.0414	-.0985	.0005	-.0004	.0003	7.64
.200	2787.2	7.73	.3998	.0559	-.1058	-.0002	-.0002	.0012	7.16
.200	2803.8	9.67	.4772	.0738	-.1107	.0003	.0000	-.0009	6.46
.201	2824.1	11.71	.5708	.1002	-.1185	.0005	.0001	-.0014	5.70
.200	2803.8	13.78	.6835	.1384	-.1306	.0007	.0001	-.0025	4.94
.201	2807.6	15.83	.7984	.1875	-.1450	.0017	.0008	-.0075	4.26
.199	2771.9	17.91	.9264	.2531	-.1610	.0007	.0003	-.0068	3.66
.201	2809.9	20.02	1.0846	.3427	-.1850	-.0018	.0015	-.0131	3.17
.201	2816.2	22.15	1.2603	.4527	-.2045	.0006	-.0028	-.0160	2.78
.200	2780.1	24.05	1.3839	.5473	-.2138	-.0012	-.0066	-.0080	2.53
.200	2791.2	-.02	.1018	.0236	-.0761	.0009	-.0000	-.0010	4.32

58 RUN 17

MACH	Q	ALPHA	CL	CD	CMS	CRMS	CYMS	CYS	L/D
	PA	DEG							
.201	2807.5	-.03	.0278	.0187	-.0355	.0006	.0006	-.0011	1.49
.200	2805.6	-1.84	-.0469	.0239	-.0292	.0004	.0008	-.0019	-1.96
.201	2823.1	.03	.0304	.0187	-.0357	.0004	.0006	-.0011	1.63
.201	2807.2	1.92	.1039	.0172	-.0425	.0002	.0002	-.0007	6.04
.201	2809.2	3.83	.1738	.0206	-.0496	.0003	-.0000	.0003	8.42
.200	2798.1	5.72	.2394	.0281	-.0559	.0004	-.0001	-.0001	8.53
.200	2795.0	7.73	.3210	.0399	-.0625	-.0001	.0000	.0000	8.04
.201	2810.2	9.70	.4007	.0557	-.0675	.0000	.0001	-.0001	7.19
.201	2808.7	11.73	.4949	.0802	-.0755	-.0000	.0002	-.0002	6.17
.200	2798.4	13.75	.6020	.1136	-.0862	.0009	.0004	-.0029	5.30
.200	2792.9	15.79	.7190	.1598	-.1003	.0018	.0015	-.0079	4.50
.200	2790.5	17.90	.8426	.2209	-.1146	.0008	.0007	-.0077	3.81
.199	2778.4	19.91	.9906	.3004	-.1346	-.0018	.0014	-.0128	3.30
.200	2806.1	22.12	1.1590	.4047	-.1518	.0006	-.0017	-.0173	2.86
.201	2822.3	24.06	1.3001	.5041	-.1640	-.0014	-.0056	-.0075	2.58
.200	2800.1	-.04	.0281	.0186	-.0354	.0007	.0006	-.0017	1.51

RUN 18

MACH	Q	ALPHA	CL	CD	CMS	CRMS	CYMS	CYS	L/D
	PA	DEG							
.200	2802.2	-.00	.0625	.0107	-.0355	.0003	.0002	-.0002	5.87
.200	2796.0	-1.78	.0188	.0096	-.0287	.0001	.0002	-.0002	1.96
.201	2811.9	.05	.0660	.0108	-.0358	.0003	.0002	.0006	6.12
.202	2834.8	1.93	.1138	.0134	-.0435	.0004	.0001	-.0002	8.51
.200	2794.7	3.81	.1687	.0190	-.0529	.0008	.0002	.0002	8.90
.201	2817.1	5.67	.2310	.0298	-.0643	.0006	.0005	-.0000	7.74
.200	2789.7	7.66	.3066	.0462	-.0792	.0006	.0010	-.0010	6.63
.201	2815.5	9.57	.3839	.0675	-.0943	.0008	.0012	-.0028	5.69
.200	2799.1	11.58	.4721	.0977	-.1128	.0024	-.0004	-.0027	4.83
.201	2827.9	13.59	.5746	.1376	-.1311	.0022	.0005	-.0064	4.18
.200	2776.3	15.61	.6719	.1846	-.1464	.0025	.0000	-.0052	3.64
.201	2809.5	17.70	.7674	.2394	-.1618	.0036	-.0013	-.0050	3.21
.201	2814.5	19.65	.8655	.3005	-.1777	.0039	-.0014	-.0056	2.88
.200	2794.0	21.74	.9660	.3724	-.1941	.0037	-.0024	-.0063	2.59
.200	2794.0	23.74	1.0643	.4511	-.2105	.0031	-.0031	-.0068	2.36
.201	2805.0	.03	.0640	.0105	-.0356	.0004	.0004	-.0004	6.11

## NASA Langley

## 7 X 10 HIGH SPEED TUNNEL

58 RUN 19

MACH	Q	ALPHA PA	CL	CD	CMS	CRMS	CYMS	CYS	L/D
		DEG							
.200	2801.9	.02	.1329	.0169	-.0754	.0005	.0002	-.0008	7.87
.201	2810.2	-1.74	.0899	.0138	-.0685	.0001	.0004	-.0006	6.52
.200	2797.1	.04	.1342	.0170	-.0755	.0003	.0004	-.0007	7.89
.201	2802.3	1.93	.1840	.0219	-.0840	.0006	.0004	-.0006	8.40
.200	2787.7	3.81	.2407	.0301	-.0955	.0009	.0001	-.0009	8.00
.200	2793.9	5.74	.3111	.0448	-.1100	.0010	.0007	-.0018	6.95
.201	2803.5	7.67	.3853	.0635	-.1257	.0010	.0012	-.0025	6.06
.201	2804.8	9.56	.4668	.0887	-.1431	.0013	.0010	-.0046	5.26
.200	2799.9	11.59	.5587	.1231	-.1628	.0026	-.0004	-.0040	4.54
.200	2787.4	13.62	.6526	.1650	-.1795	.0026	.0005	-.0065	3.96
.201	2802.9	15.64	.7482	.2146	-.1947	.0030	-.0003	-.0058	3.49
.201	2815.5	17.74	.8576	.2769	-.2122	.0035	-.0011	-.0060	3.10
.200	2801.0	19.68	.9537	.3414	-.2278	.0039	-.0015	-.0055	2.79
.201	2826.1	21.77	1.0551	.4177	-.2446	.0038	-.0024	-.0065	2.53
.200	2792.6	23.77	1.1488	.4988	-.2595	.0029	-.0026	-.0064	2.30
.200	2795.4	.02	.1362	.0168	-.0759	.0004	.0005	-.0005	8.13

58 RUN 20

MACH	Q	ALPHA PA	CL	CD	CMS	CRMS	CYMS	CYS	L/D
		DEG							
.200	2784.3	.01	.0186	.0088	-.0072	.0002	.0000	-.0006	2.12
.200	2791.7	-1.76	-.0232	.0092	-.0007	.0005	.0001	-.0003	-2.52
.200	2790.4	.03	.0197	.0090	-.0073	.0002	.0000	-.0002	2.18
.201	2805.8	1.90	.0688	.0103	-.0150	.0005	.0001	.0002	6.66
.201	2810.0	3.78	.1179	.0140	-.0220	.0009	-.0002	.0005	8.42
.200	2788.8	5.66	.1768	.0227	-.0309	.0004	.0002	-.0004	7.79
.201	2799.1	7.65	.2492	.0365	-.0443	.0009	.0007	-.0012	6.82
.200	2792.3	9.56	.3285	.0562	-.0587	.0009	.0010	-.0031	5.84
.200	2788.7	11.57	.4145	.0835	-.0758	.0023	-.0008	-.0020	4.97
.200	2779.8	13.57	.5092	.1196	-.0933	.0024	.0000	-.0056	4.26
.200	2792.9	15.60	.6081	.1640	-.1090	.0023	-.0007	-.0045	3.71
.200	2776.4	17.71	.7136	.2196	-.1253	.0030	-.0018	-.0049	3.25
.200	2775.6	19.64	.8096	.2779	-.1409	.0036	-.0024	-.0048	2.91
.201	2811.0	21.76	.9134	.3495	-.1577	.0030	-.0028	-.0058	2.61
.200	2795.8	23.73	1.0149	.4271	-.1738	.0030	-.0036	-.0052	2.38
.200	2780.1	.01	.0202	.0088	-.0073	.0004	-.0002	-.0000	2.31

58 RUN 21

MACH	Q	ALPHA PA	CL	CD	CMS	CRMS	CYMS	CYS	L/D
		DEG							
.200	2792.0	.02	.1929	.0286	-.1100	.0003	.0003	-.0010	6.75
.200	2779.2	-1.76	.1470	.0236	-.1022	.0001	.0005	-.0009	6.23
.200	2791.0	.04	.1958	.0286	-.1103	.0005	.0003	-.0006	6.86
.201	2797.7	1.93	.2450	.0356	-.1191	.0011	.0003	-.0010	6.88
.201	2802.8	3.80	.3106	.0476	-.1348	.0013	-.0001	-.0009	6.53
.200	2787.5	5.69	.3810	.0649	-.1514	.0016	.0006	-.0021	5.87
.200	2779.1	7.67	.4631	.0891	-.1704	.0015	.0012	-.0034	5.20
.201	2800.7	9.57	.5473	.1180	-.1900	.0019	.0000	-.0027	4.64
.200	2775.4	11.61	.6419	.1566	-.2103	.0028	-.0007	-.0023	4.10
.201	2802.1	13.66	.7439	.2046	-.2293	.0030	-.0001	-.0056	3.64
.201	2804.2	15.64	.8394	.2575	-.2456	.0031	-.0008	-.0053	3.26
.201	2805.7	17.74	.9356	.3200	-.2610	.0034	-.0016	-.0063	2.92
.201	2815.8	19.71	1.0494	.3951	-.2821	.0042	-.0023	-.0063	2.66
.201	2801.8	21.79	1.1329	.4686	-.2925	.0028	-.0025	-.0056	2.42
.201	2801.4	23.77	1.2293	.5538	-.3087	.0023	-.0031	-.0056	2.22
.201	2812.5	.03	.1979	.0286	-.1110	.0004	.0002	-.0007	6.92

## NASA Langley

## 7 X 10 HIGH SPEED TUNNEL

58 RUN 22

MACH	Q	ALPHA	CL	CD	CMS	CRMS	CYMS	CYS	L/D
PA		DEG							
.200	2790.9	.01	.1737	.0322	-.1077	.0003	.0001	-.0013	5.40
.201	2798.4	-1.81	.1077	.0320	-.0996	.0002	.0004	-.0015	3.36
.201	2794.7	.04	.1768	.0325	-.1084	.0005	.0002	-.0009	5.45
.201	2812.2	1.92	.2450	.0369	-.1191	.0007	.0002	-.0010	6.65
.200	2777.1	3.86	.3170	.0469	-.1330	.0008	-.0002	-.0005	6.76
.200	2780.0	5.70	.3903	.0607	-.1476	.0007	-.0001	-.0011	6.44
.200	2768.2	7.71	.4676	.0777	-.1603	.0002	-.0003	-.0013	6.02
.201	2807.7	9.60	.5352	.0962	-.1680	.0000	-.0001	-.0011	5.56
.200	2774.0	11.63	.6103	.1205	-.1779	.0003	.0003	-.0020	5.06
.200	2771.1	13.68	.6987	.1515	-.1916	.0002	.0004	-.0028	4.61
.201	2798.5	15.68	.7977	.1941	-.2085	.0011	-.0010	-.0045	4.11
.200	2788.7	17.79	.9394	.2693	-.2389	.0004	-.0018	-.0054	3.49
.201	2801.7	19.80	1.1533	.3889	-.2939	.0009	-.0052	.0045	2.97
.200	2779.5	22.02	1.3234	.5100	-.3081	-.0034	-.0018	.0073	2.59
.200	2771.7	24.03	1.4449	.6148	-.3147	-.0013	-.0022	.0000	2.35
.199	2762.7	.02	.1764	.0324	-.1086	.0005	.0002	-.0012	5.45

58 RUN 23

MACH	Q	ALPHA	CL	CD	CMS	CRMS	CYMS	CYS	L/D
PA		DEG							
.201	2800.2	-.02	-.0162	.0154	-.0002	.0005	.0002	-.0000	-1.05
.200	2782.8	-1.84	-.0898	.0209	.0110	.0005	.0004	-.0004	-4.30
.201	2801.7	.00	-.0168	.0152	-.0002	.0005	.0003	-.0004	-1.11
.200	2774.4	1.88	.0573	.0137	-.0117	.0005	.0005	-.0006	4.19
.200	2792.3	3.80	.1219	.0158	-.0210	.0002	.0001	.0007	7.73
.200	2787.6	5.67	.1829	.0213	-.0290	.0003	.0002	.0007	8.58
.200	2784.1	7.68	.2577	.0307	-.0389	.0001	.0002	.0008	6.40
.201	2794.8	9.58	.3258	.0429	-.0470	.0006	.0002	-.0005	7.60
.200	2784.1	11.59	.4001	.0593	-.0560	.0009	.0004	-.0015	6.75
.200	2781.7	13.60	.4885	.0840	-.0703	.0004	.0011	-.0009	5.82
.202	2822.3	15.65	.5971	.1213	-.0883	.0008	-.0000	-.0025	4.92
.200	2767.3	17.72	.7143	.1786	-.1063	.0010	-.0005	-.0048	4.00
.201	2805.9	19.73	.8679	.2614	-.1397	.0008	-.0001	-.0086	3.32
.200	2775.3	21.94	1.0625	.3769	-.1659	.0022	-.0024	-.0058	2.82
.201	2799.6	23.96	1.1933	.4746	-.1739	.0011	-.0031	-.0048	2.51
.201	2794.8	-.03	-.0178	.0153	-.0002	.0003	.0003	-.0006	-1.17

58 RUN 24

MACH	Q	ALPHA	CL	CD	CMS	CRMS	CYMS	CYS	L/D
PA		DEG							
.200	2810.1	.02	.0129	.0268	.0003	.0001	-.0000	.0006	.48
.200	2811.7	-1.80	-.0604	.0292	.0102	.0005	-.0002	.0002	-2.07
.201	2818.8	.01	.0121	.0264	.0002	.0000	.0000	.0003	.46
.201	2822.0	1.94	.0923	.0271	-.0113	.0001	.0002	.0006	3.41
.201	2819.3	3.84	.1660	.0320	-.0218	-.0003	.0000	.0014	5.19
.200	2813.9	5.75	.2472	.0401	-.0331	.0003	.0000	.0004	6.16
.200	2807.5	7.75	.3365	.0539	-.0453	.0008	-.0001	.0010	6.25
.200	2815.0	9.71	.4233	.0709	-.0558	.0008	-.0004	.0016	5.97
.201	2819.5	11.72	.5199	.0945	-.0672	.0005	-.0002	.0015	5.50
.200	2809.6	13.79	.6220	.1261	-.0794	-.0003	-.0008	.0004	4.93
.200	2817.0	15.83	.7262	.1672	-.0924	.0009	-.0023	-.0019	4.34
.200	2798.0	17.88	.8321	.2191	-.1049	-.0004	-.0047	-.0006	3.80
.200	2799.1	19.86	.9395	.2800	-.1198	-.0011	-.0047	-.0035	3.36
.200	2798.8	22.01	1.0540	.3587	-.1303	-.0016	-.0051	-.0068	2.94
.200	2806.8	23.77	1.1253	.4270	-.1372	-.0072	-.0082	.0034	2.64
.200	2805.6	.02	.0127	.0265	-.0000	-.0002	-.0002	.0003	.48

## NASA Langley

## 7 X 10 HIGH SPEED TUNNEL

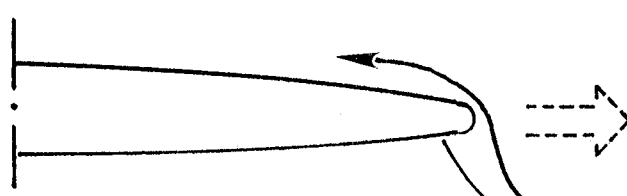
58 RUN 25

MACH	Q	ALPHA	CL	CD	CMS	CRMS	CYMS	CYS	L/D
	PA	DEG							
.200	2808.9	.05	.2786	.0633	-.1457	-.0007	-.0008	.0016	4.40
.201	2817.1	-1.77	.2038	.0572	-.1337	-.0008	-.0009	.0012	3.56
.201	2816.5	.04	.2796	.0634	-.1458	-.0008	-.0008	.0019	4.41
.200	2806.5	1.97	.3594	.0746	-.1591	-.0007	-.0011	.0025	4.82
.200	2789.9	3.90	.4400	.0897	-.1729	-.0002	-.0012	.0027	4.91
.201	2829.2	5.79	.5256	.1095	-.1880	-.0002	-.0016	.0032	4.80
.200	2799.7	7.80	.6266	.1365	-.2075	-.0003	-.0018	.0034	4.59
.200	2799.0	9.74	.7285	.1680	-.2258	-.0007	-.0014	.0034	4.34
.200	2805.4	11.82	.8342	.2054	-.2422	-.0018	-.0014	.0033	4.06
.201	2830.1	13.83	.9367	.2466	-.2550	-.0024	-.0011	.0016	3.80
.201	2817.2	15.87	1.0403	.2975	-.2679	-.0015	-.0027	.0002	3.50
.200	2790.6	17.96	1.1472	.3617	-.2826	-.0037	-.0046	.0014	3.17
.199	2775.2	19.97	1.2654	.4413	-.3007	-.0056	-.0046	.0004	2.87
.200	2808.1	22.07	1.3696	.5266	-.3106	-.0060	-.0053	-.0029	2.60
.200	2809.1	23.84	1.4207	.5956	-.3027	-.0078	-.0071	.0002	2.39
.201	2816.6	.05	.2824	.0632	-.1462	-.0009	-.0007	.0011	4.47

58 RUN 26

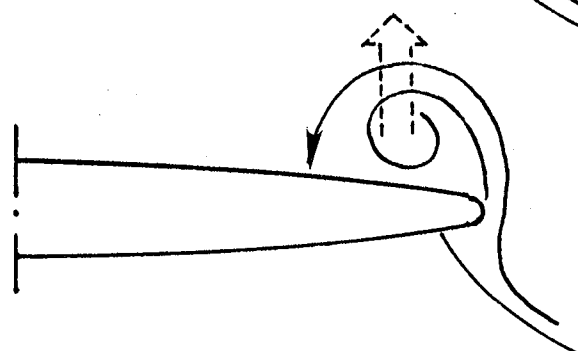
MACH	Q	ALPHA	CL	CD	CMS	CRMS	CYMS	CYS	L/D
	PA	DEG							
.200	2809.3	.05	.2449	.0490	-.1274	.0001	.0002	.0000	4.99
.201	2831.1	-1.77	.1694	.0445	-.1167	.0002	.0000	.0002	3.81
.201	2821.2	.08	.2472	.0489	-.1281	.0000	-.0001	.0006	5.06
.201	2819.7	2.01	.3256	.0580	-.1405	.0006	-.0001	.0007	5.61
.200	2807.7	3.93	.4048	.0707	-.1527	.0004	-.0006	.0020	5.72
.200	2797.1	5.80	.4907	.0881	-.1669	.0009	-.0005	.0021	5.57
.199	2785.2	7.82	.5910	.1126	-.1862	.0005	-.0008	.0025	5.25
.201	2817.0	9.74	.6837	.1388	-.1991	.0008	-.0005	.0012	4.92
.201	2817.4	11.79	.7896	.1728	-.2138	.0002	-.0005	.0014	4.57
.200	2793.3	13.81	.8960	.2152	-.2299	-.0007	-.0006	.0010	4.16
.199	2765.6	15.87	.9962	.2637	-.2412	-.0002	-.0024	-.0020	3.78
.200	2789.7	17.97	1.1100	.3280	-.2564	-.0009	-.0047	-.0016	3.38
.198	2758.7	19.93	1.2203	.4000	-.2738	-.0023	-.0051	-.0036	3.05
.200	2798.5	22.07	1.3425	.4913	-.2889	-.0037	-.0058	-.0040	2.73
.201	2820.0	23.87	1.4159	.5736	-.2917	-.0062	-.0067	-.0018	2.47
.201	2834.0	.04	.2455	.0493	-.1277	.0002	.0003	.0010	4.98

( End of Test 58 )



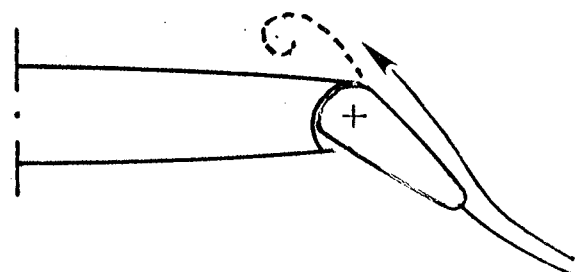
(A)

ATTACHED FLOW  
(FULL L.E. SUCTION)



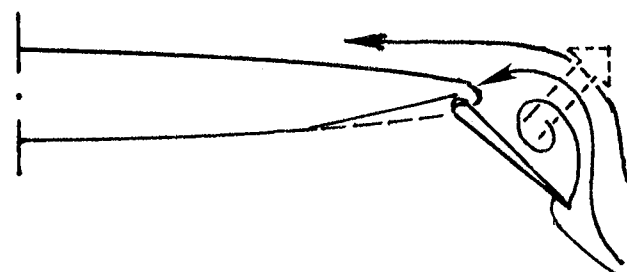
(B)

SEPARATION WITH  
L.E. VORTEX  
(ZERO SUCTION)



(C)

L.E. DROOP OR FLAP  
FOR ATTACHED FLOW



(D)

VORTEX-FLAP

FIG. I LEADING-EDGE FLOWS OVER HIGHLY SWEPT WING  
(VIEWED IN CROSS-FLOW PLANE)

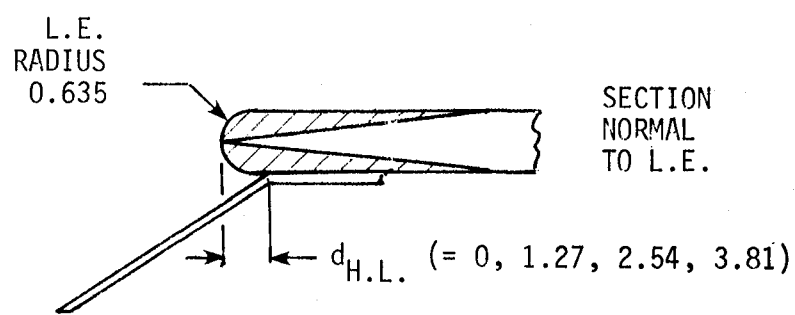
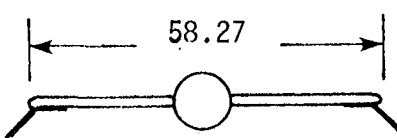
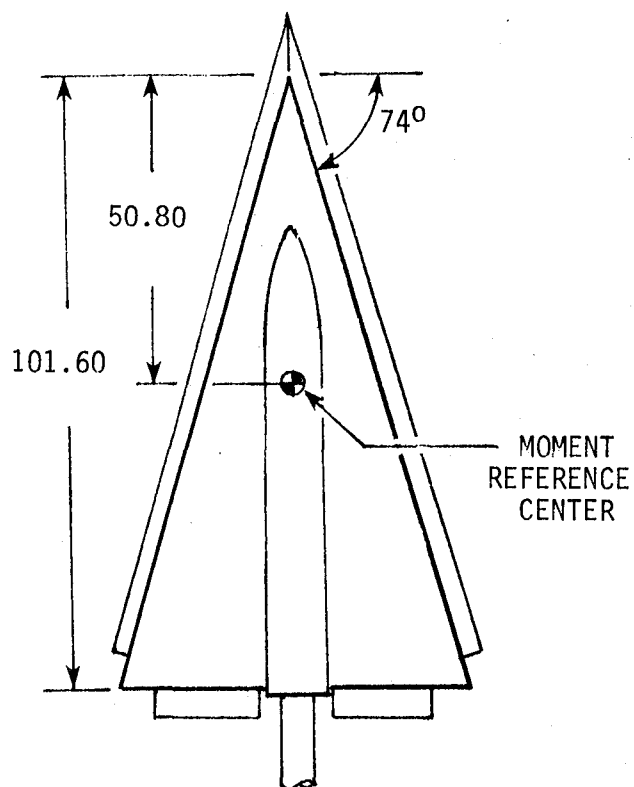
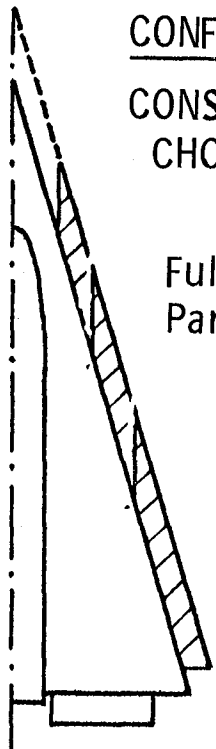


FIG. 2 TEST MODEL GEOMETRY AND DIMENSIONS (in cms)

CONFIG. # I

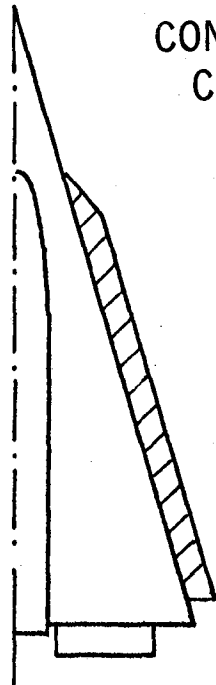
CONSTANT  
CHORD

Full Span &  
Part Span.



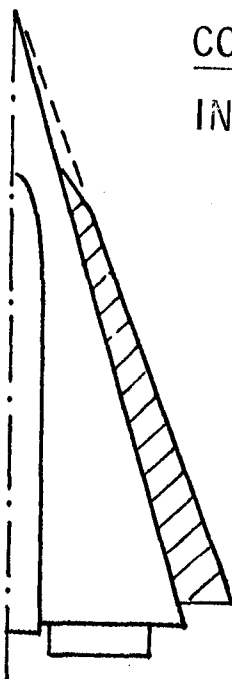
CONFIG. # II

CONSTANT  
CHORD



CONFIG. # III

INVERSE TAPER



CONFIG. # IV

EXTENDED  
FLAP

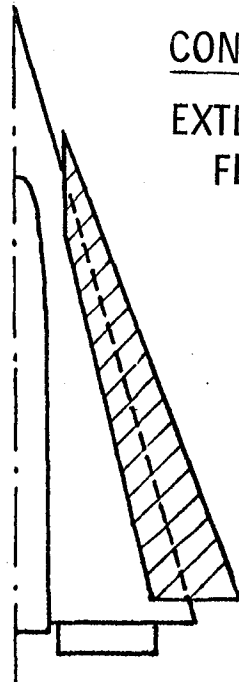


FIG.3 LEADING EDGE VORTEX-FLAP TEST CONFIGURATIONS

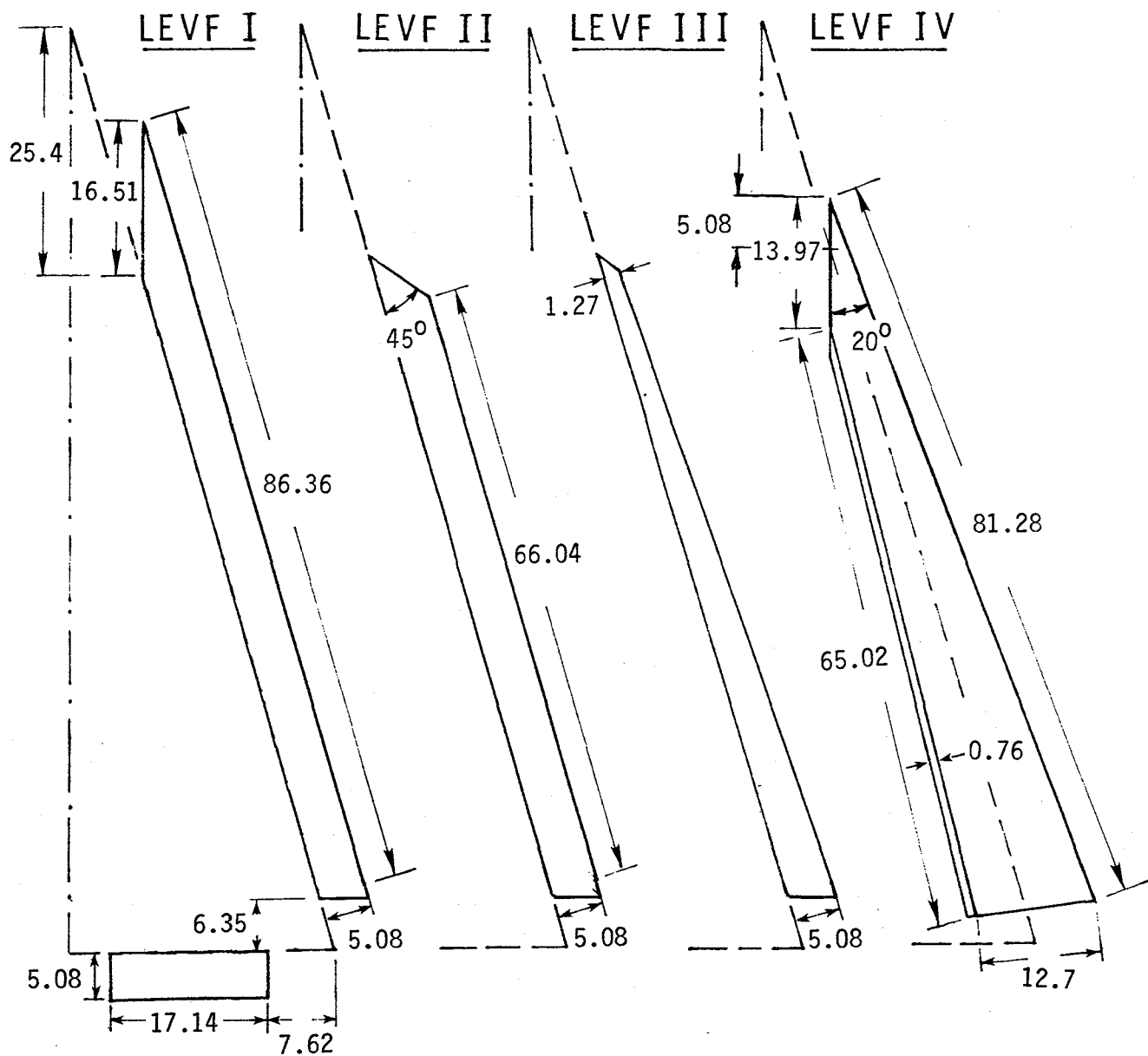


FIG.4 LEADING EDGE VORTEX-FLAP GEOMETRY AND DIMENSIONS (in cms)

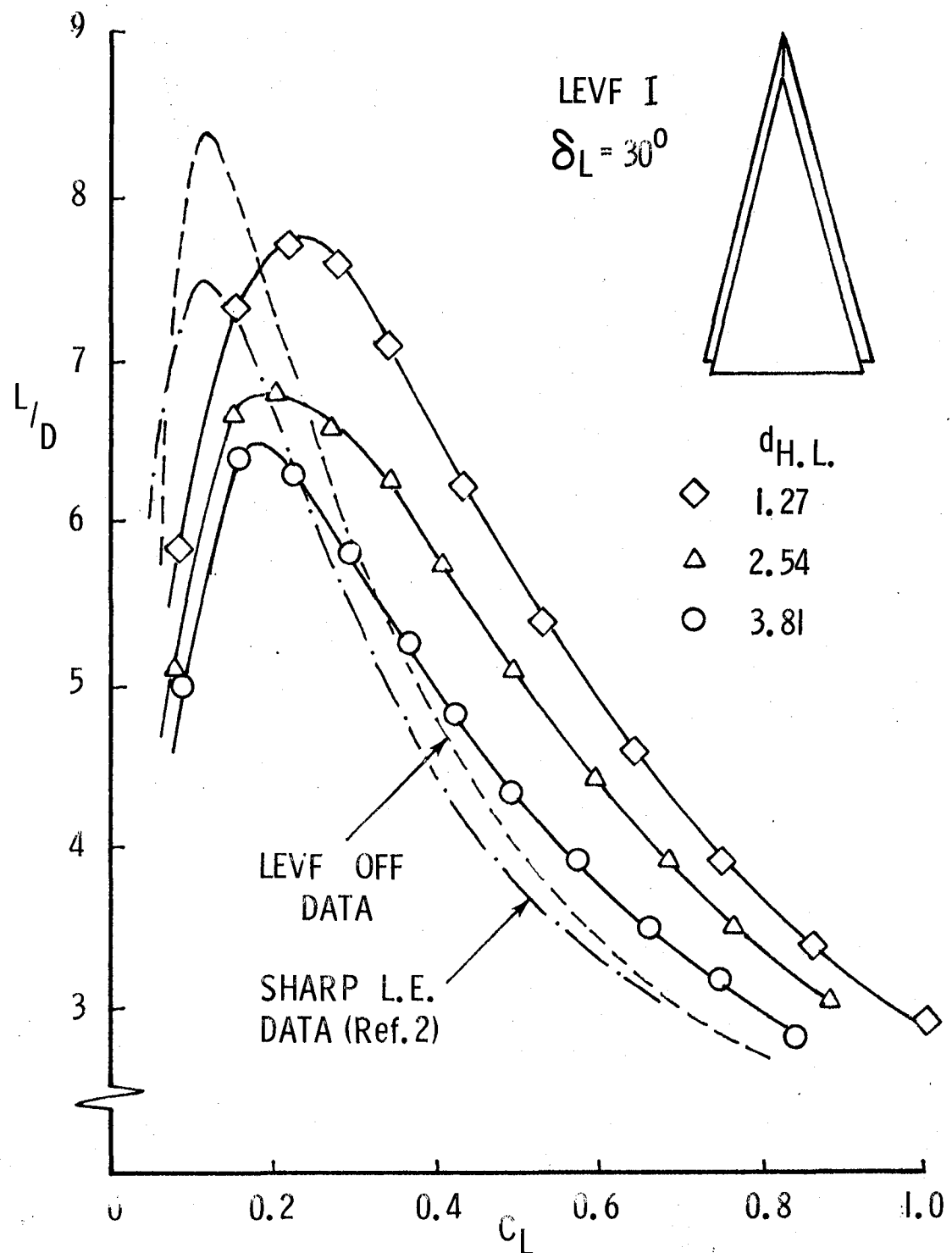
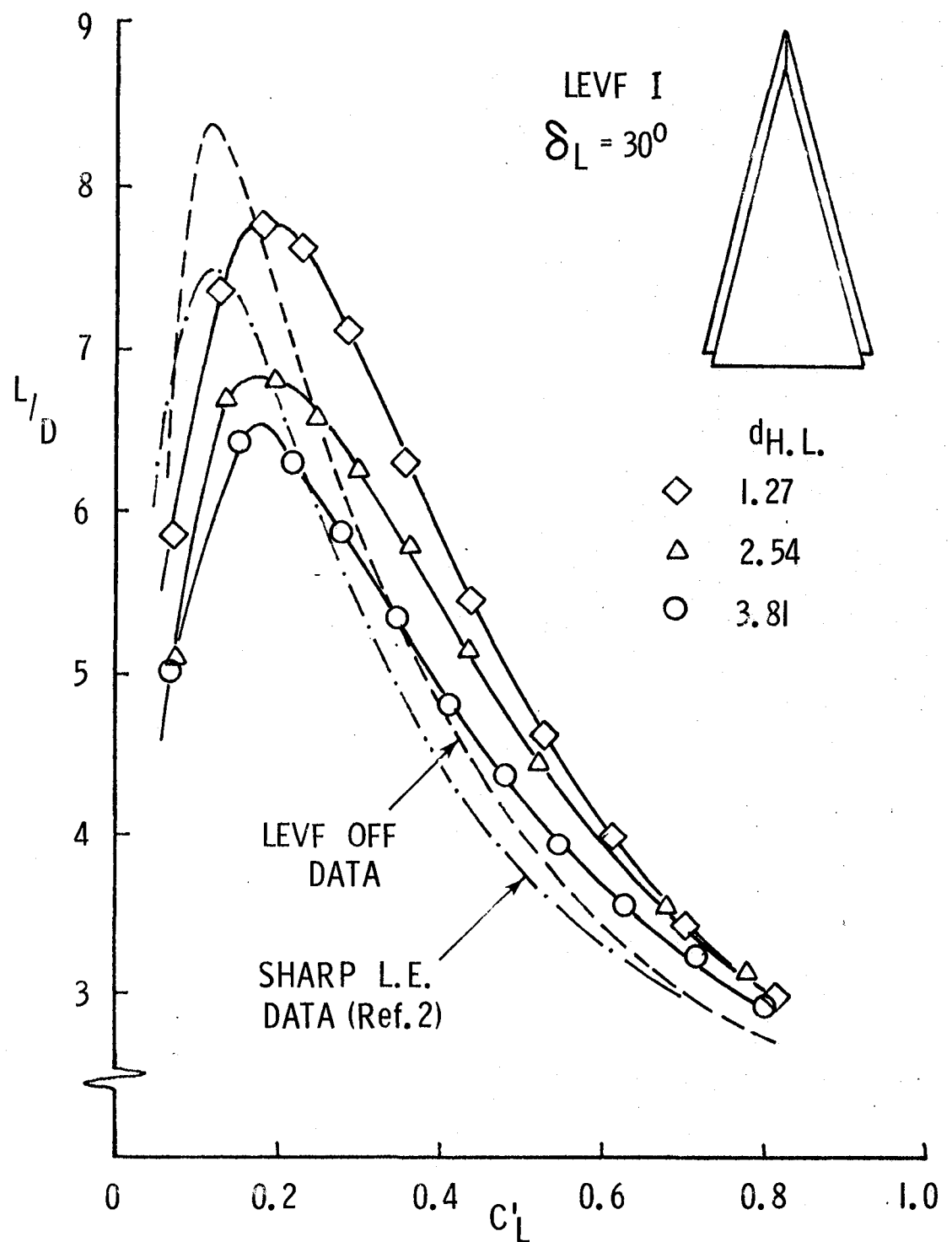


FIG. 5A EFFECT OF HINGE-LINE DISTANCE FROM LEADING-EDGE ON  $L/D$  VS.  $C_L$  CHARACTERISTICS



**FIG. 5 B** EFFECT OF HINGE-LINE DISTANCE FROM LEADING-EDGE  
 ON  $L/D$  VS.  $C_L'$  (AREA-CORRECTED) CHARACTERISTICS

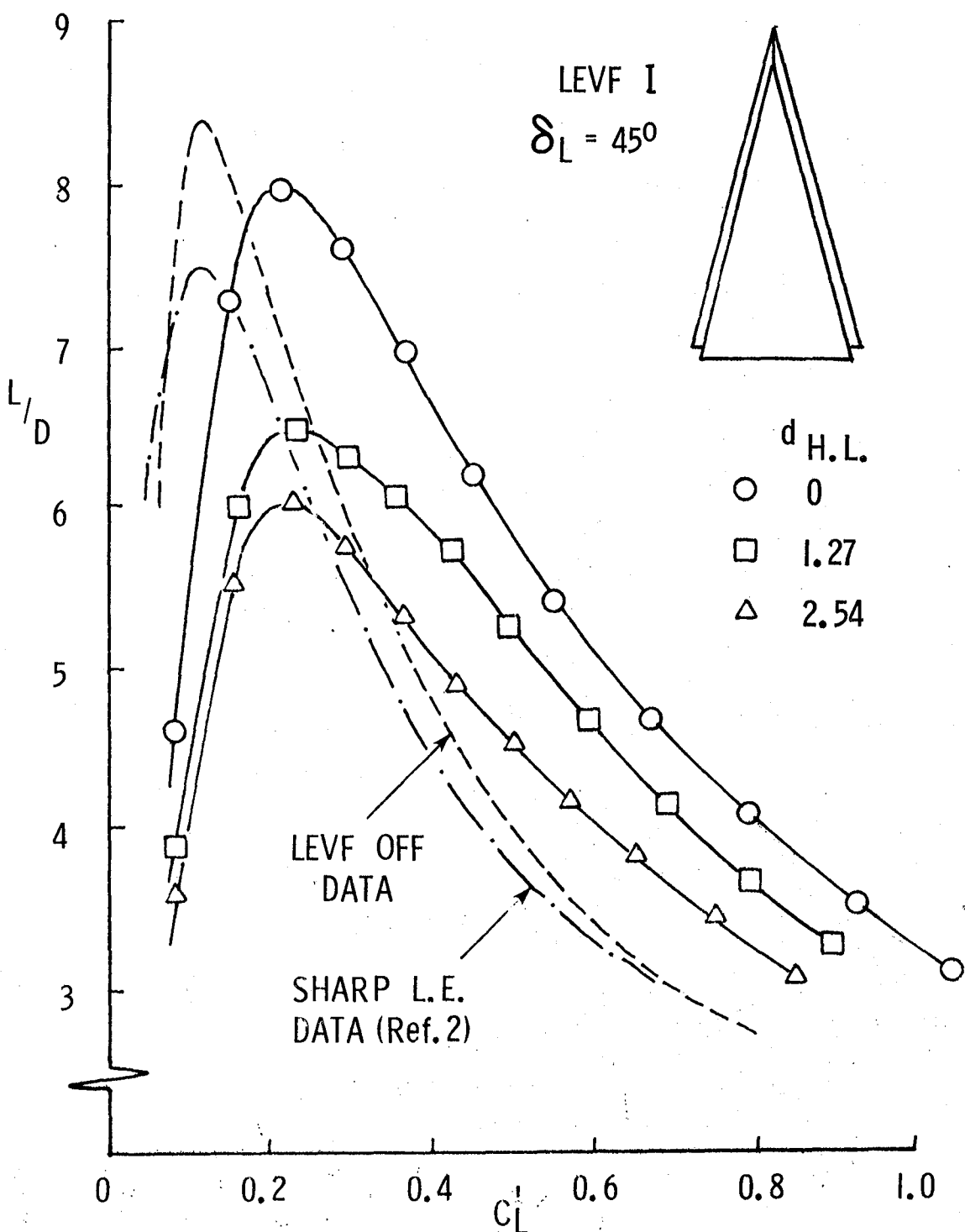


FIG. 6A EFFECT OF HINGE-LINE DISTANCE FROM LEADING-EDGE  
 ON  $L/D$  VS.  $C_L$  CHARACTERISTICS

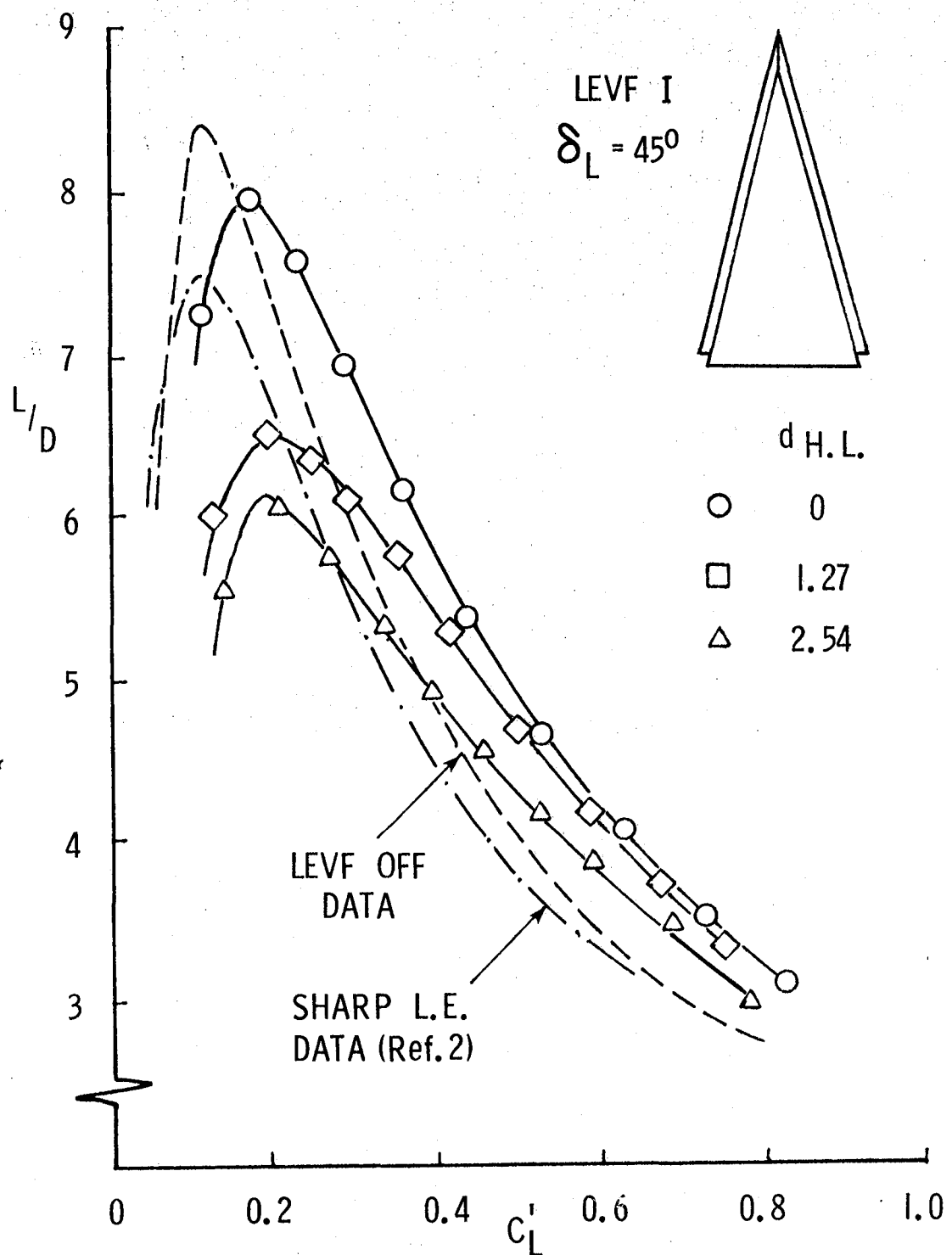


FIG. 6B EFFECT OF HINGE-LINE DISTANCE FROM LEADING-EDGE  
ON  $L/D$  VS.  $C_L'$  (AREA-CORRECTED) CHARACTERISTICS

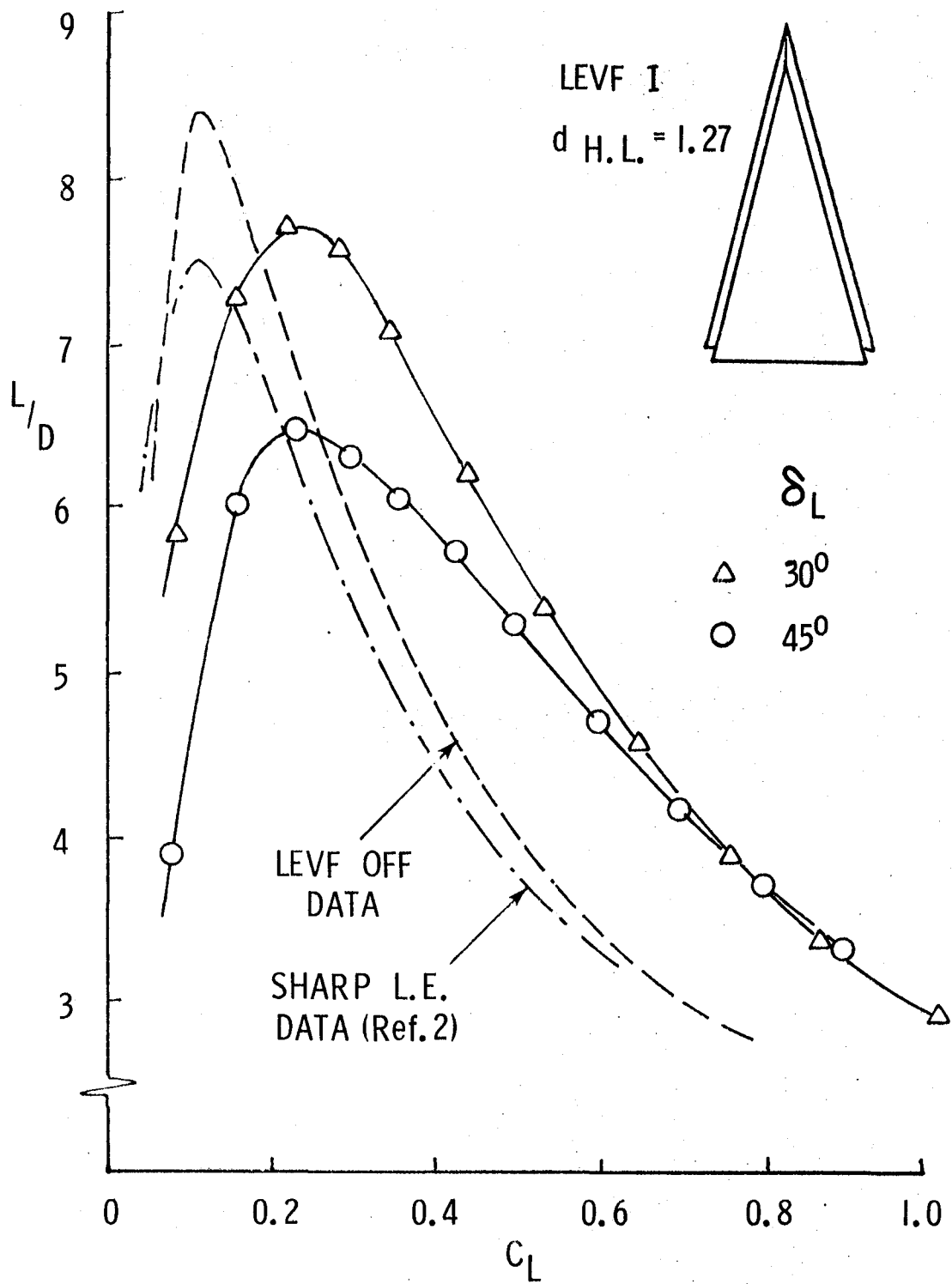


FIG. 7 A EFFECT OF FLAP DEFLECTION ANGLE ON  $L/D$  VS.  
 $C_L$  CHARACTERISTICS

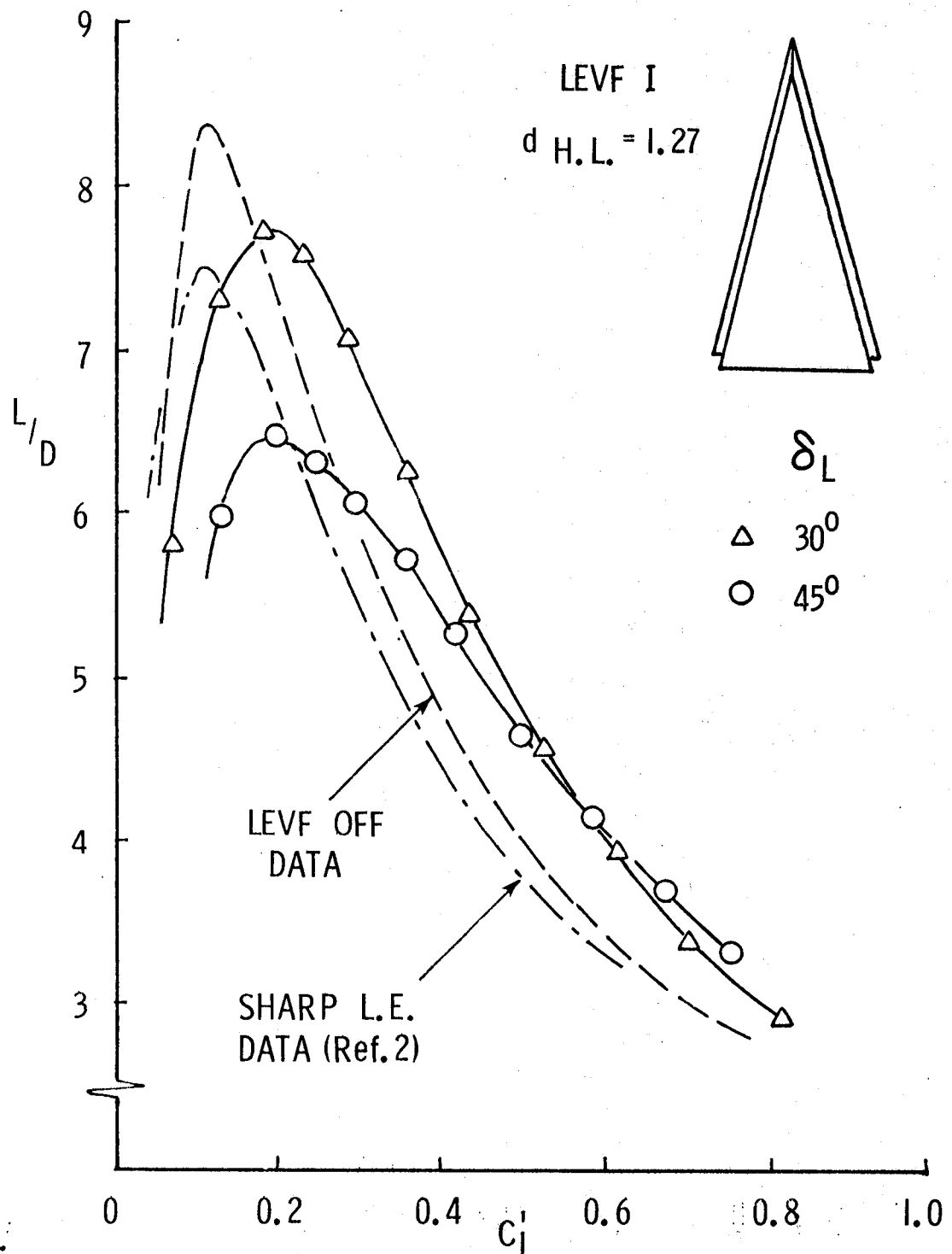


FIG. 7 B      EFFECT OF FLAP DEFLECTION ANGLE ON  $L/D$  VS.  
 $C_L$  (AREA-CORRECTED) CHARACTERISTICS

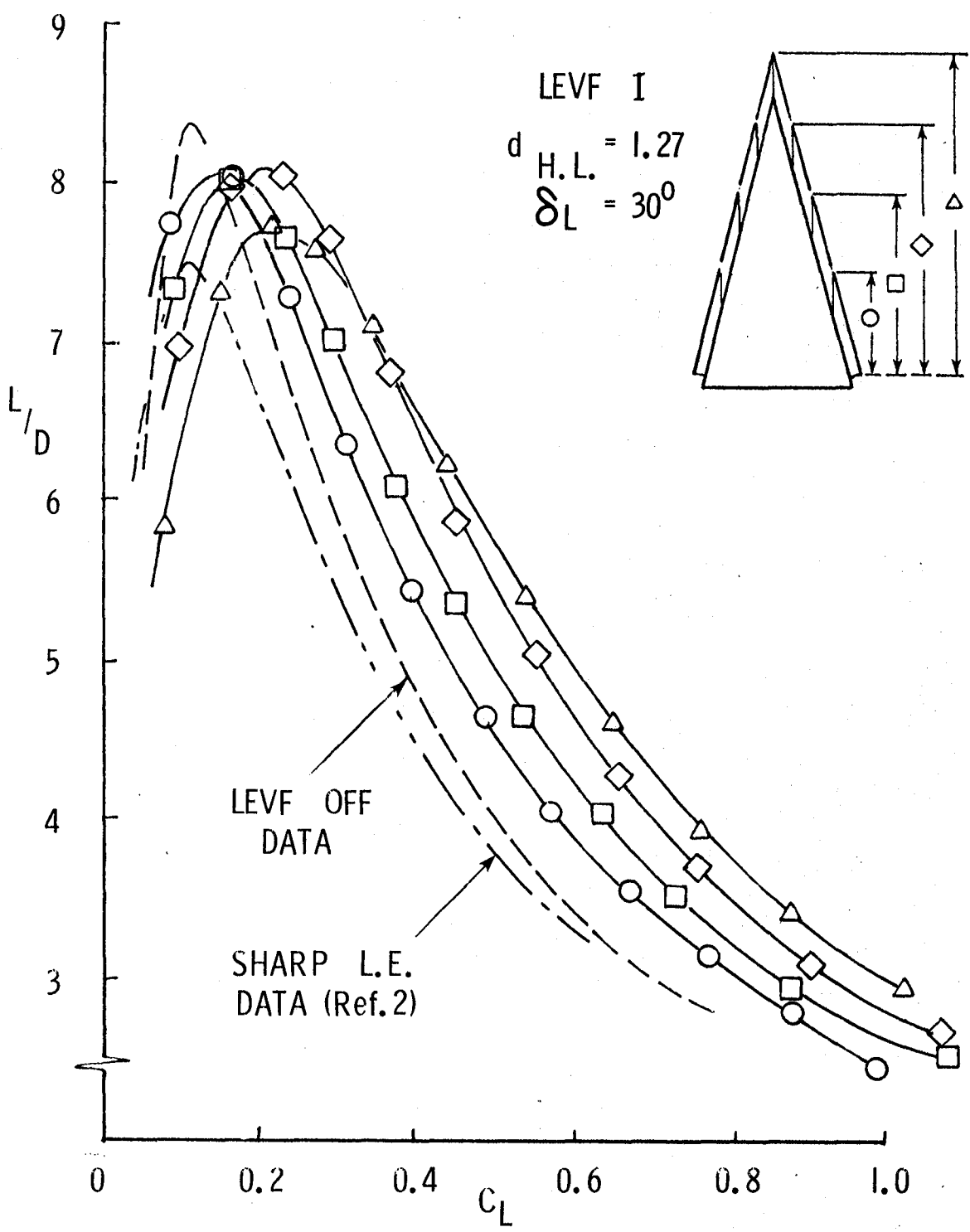


FIG. 8 A EFFECT OF PART-SPAN FLAP LENGTH ON  $L/D$  VS.  
 $C_L$  CHARACTERISTICS

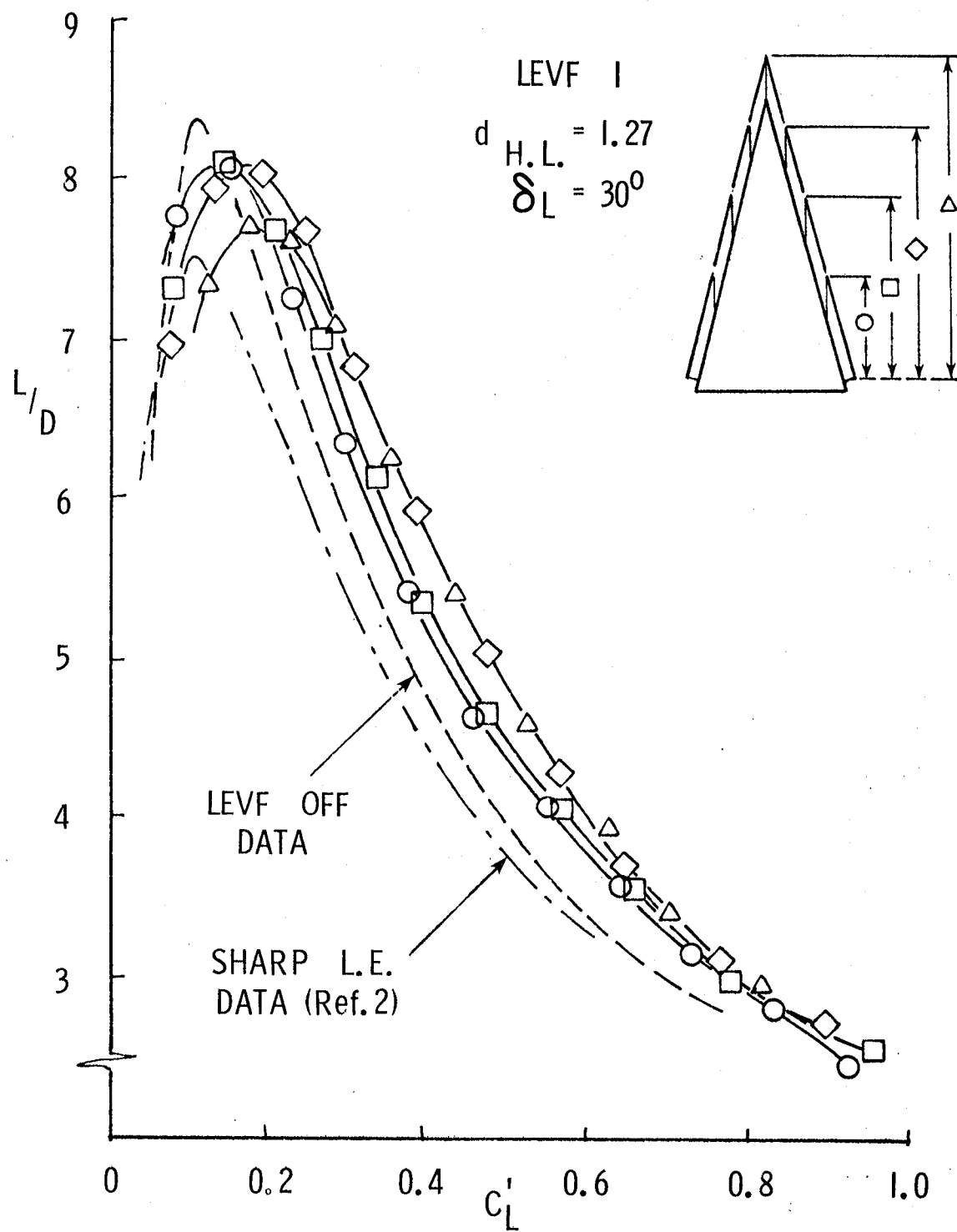


FIG. 8 B    EFFECT OF PART-SPAN FLAP LENGTH ON  $L/D$  VS.  
 $C'_L$  (AREA-CORRECTED) CHARACTERISTICS

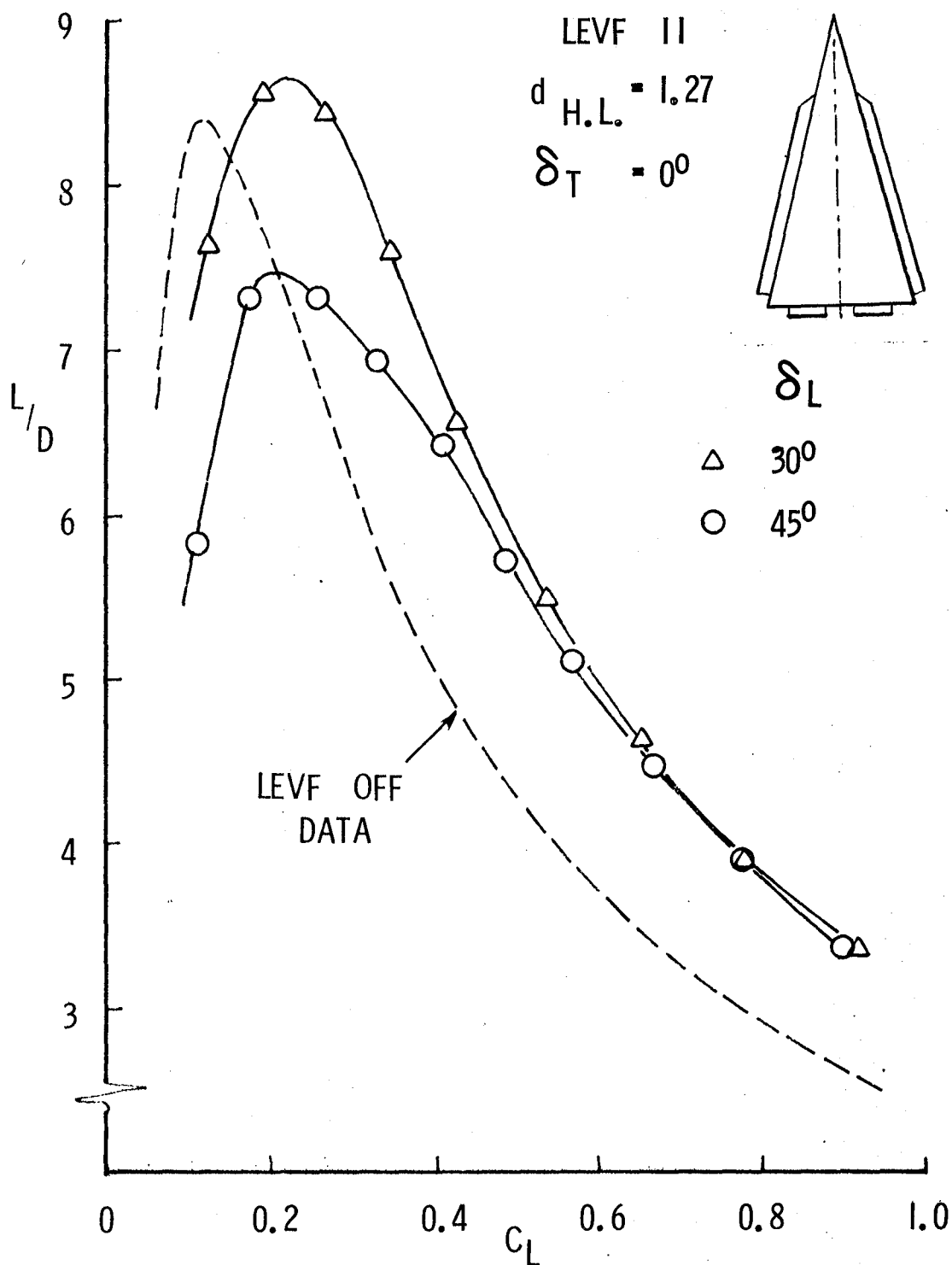


FIG. 9 EFFECT OF FLAP DEFLECTION ANGLE (PART-SPAN FLAP)  
ON  $L/D$  VS.  $C_L$  CHARACTERISTICS

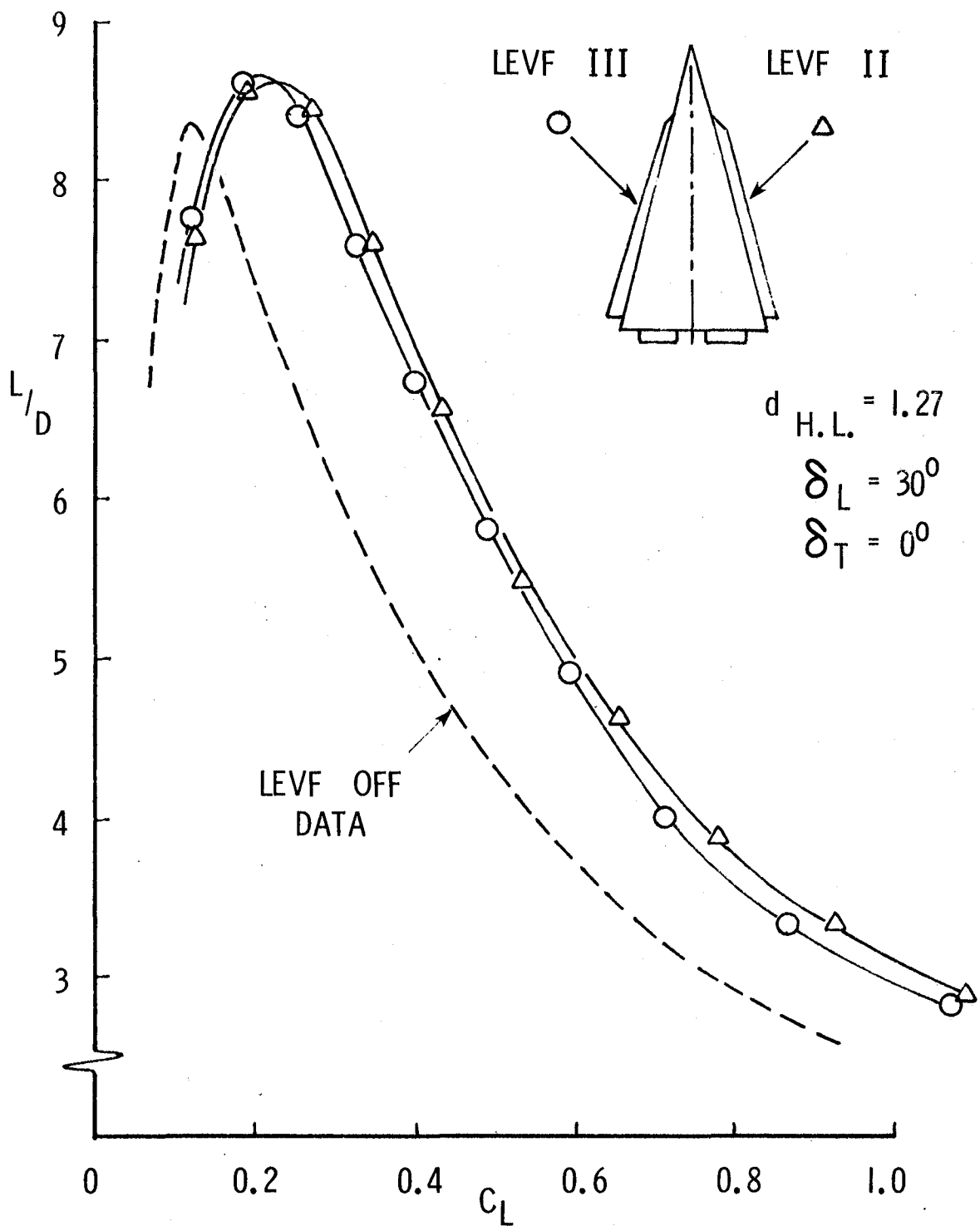
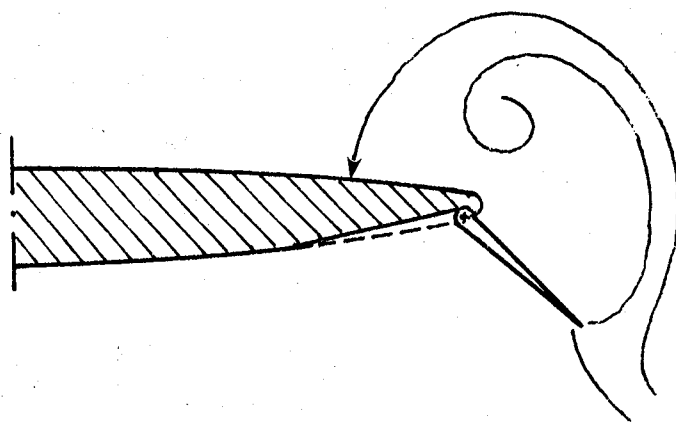
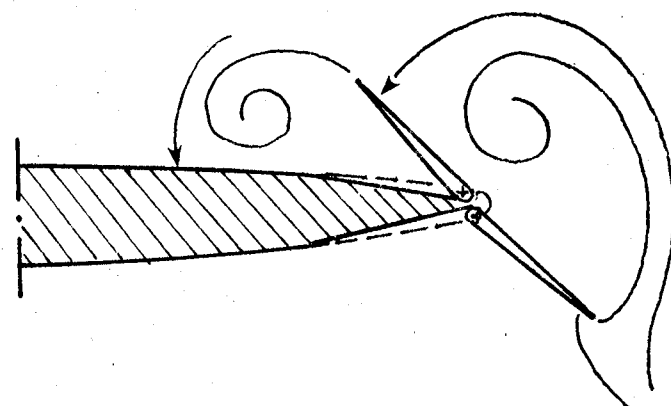


FIG. 10 COMPARISON OF CONSTANT-CHORD AND INVERSE-TAPER FLAP  $L/D$  VS.  $C_L$  CHARACTERISTICS



LOWER  
FLAP  
ONLY



UPPER  
FLAP  
ADDED

FIG. II EXTENDED FLAP CONCEPT FOR HIGH ANGLE OF ATTACK

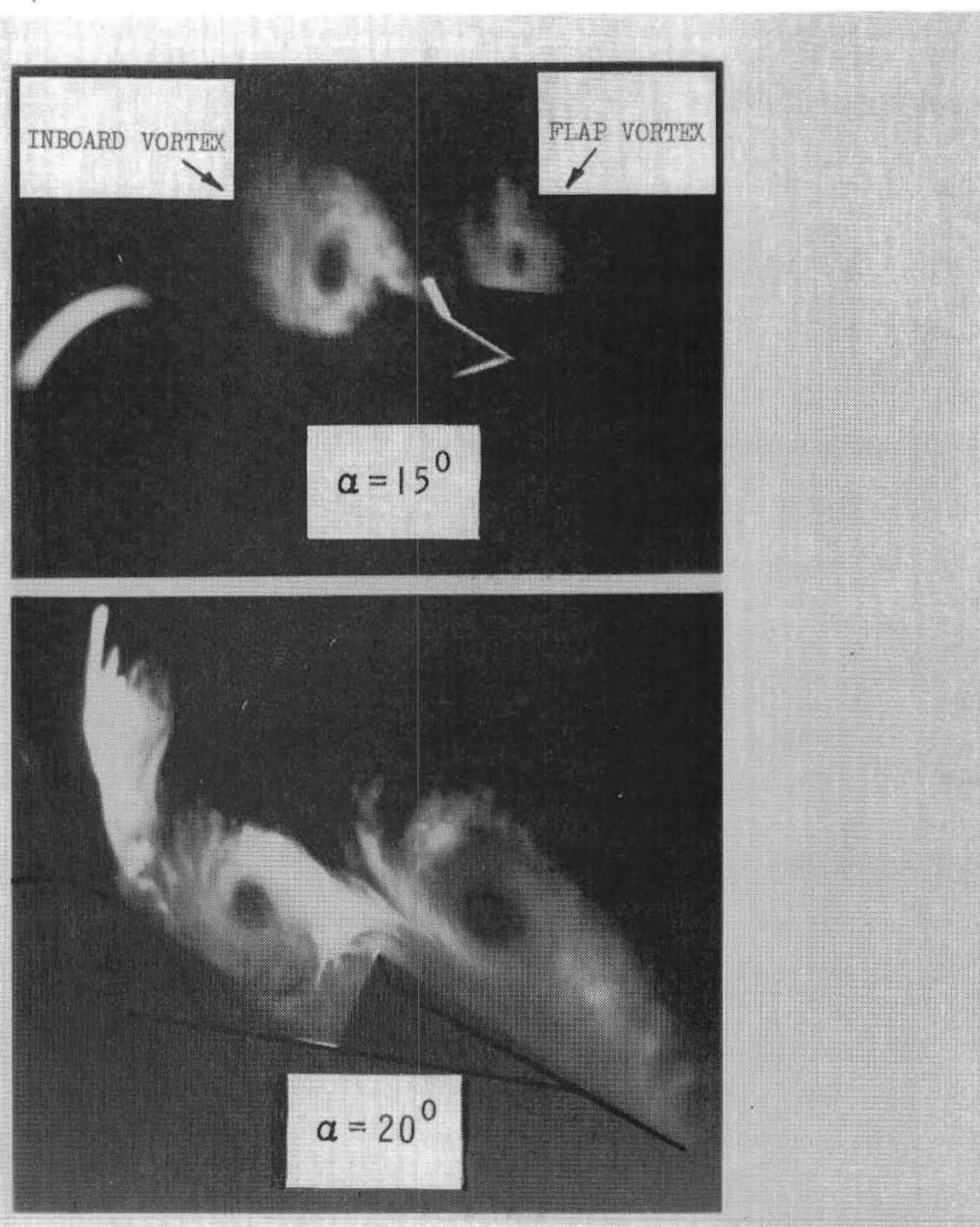


FIG. 12 SMOKE VISUALIZATION OF VORTICES ON EXTENDED FLAP

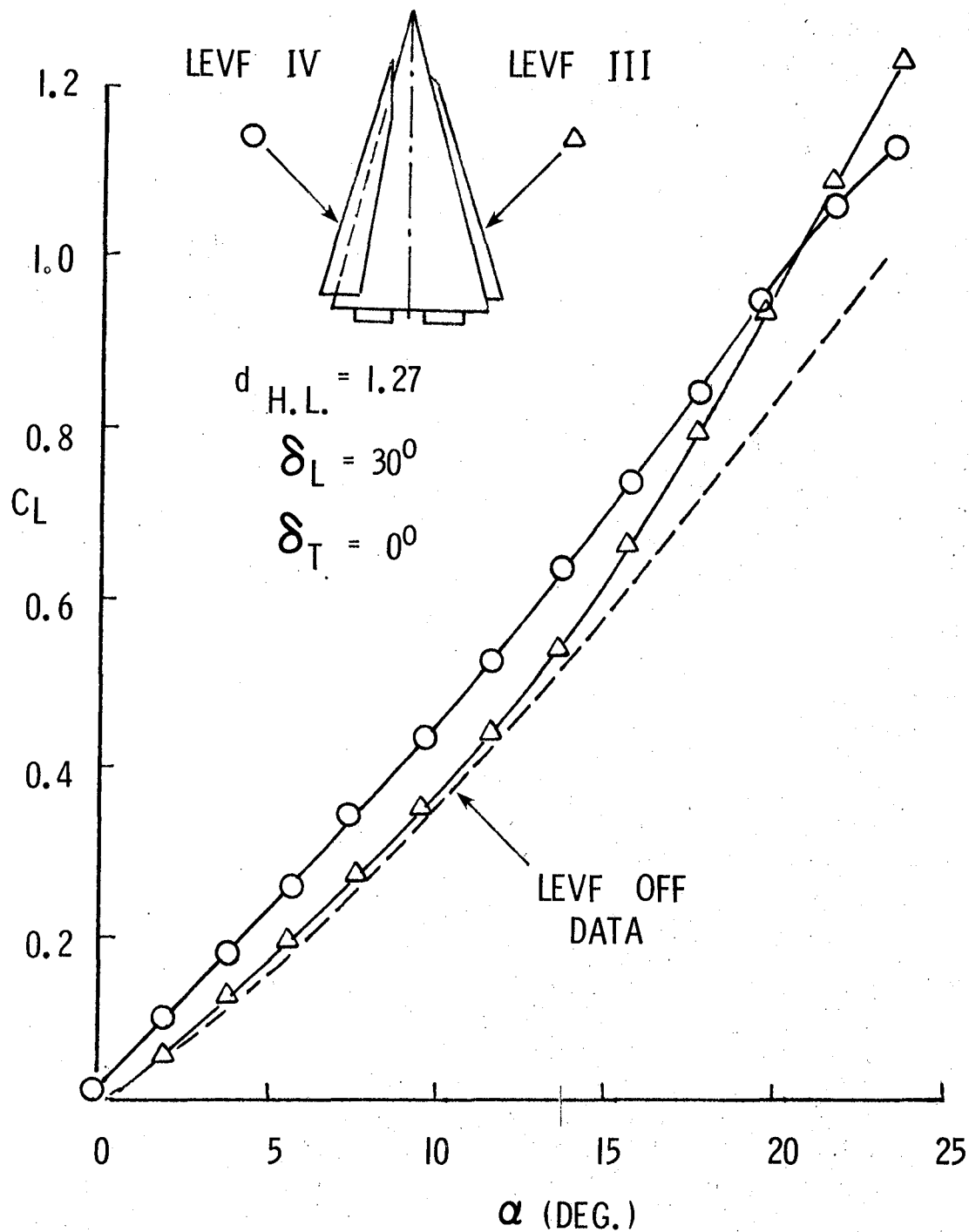


FIG. 13A COMPARISON OF INVERSE-TAPER AND EXTENDED FLAP LIFT CHARACTERISTICS

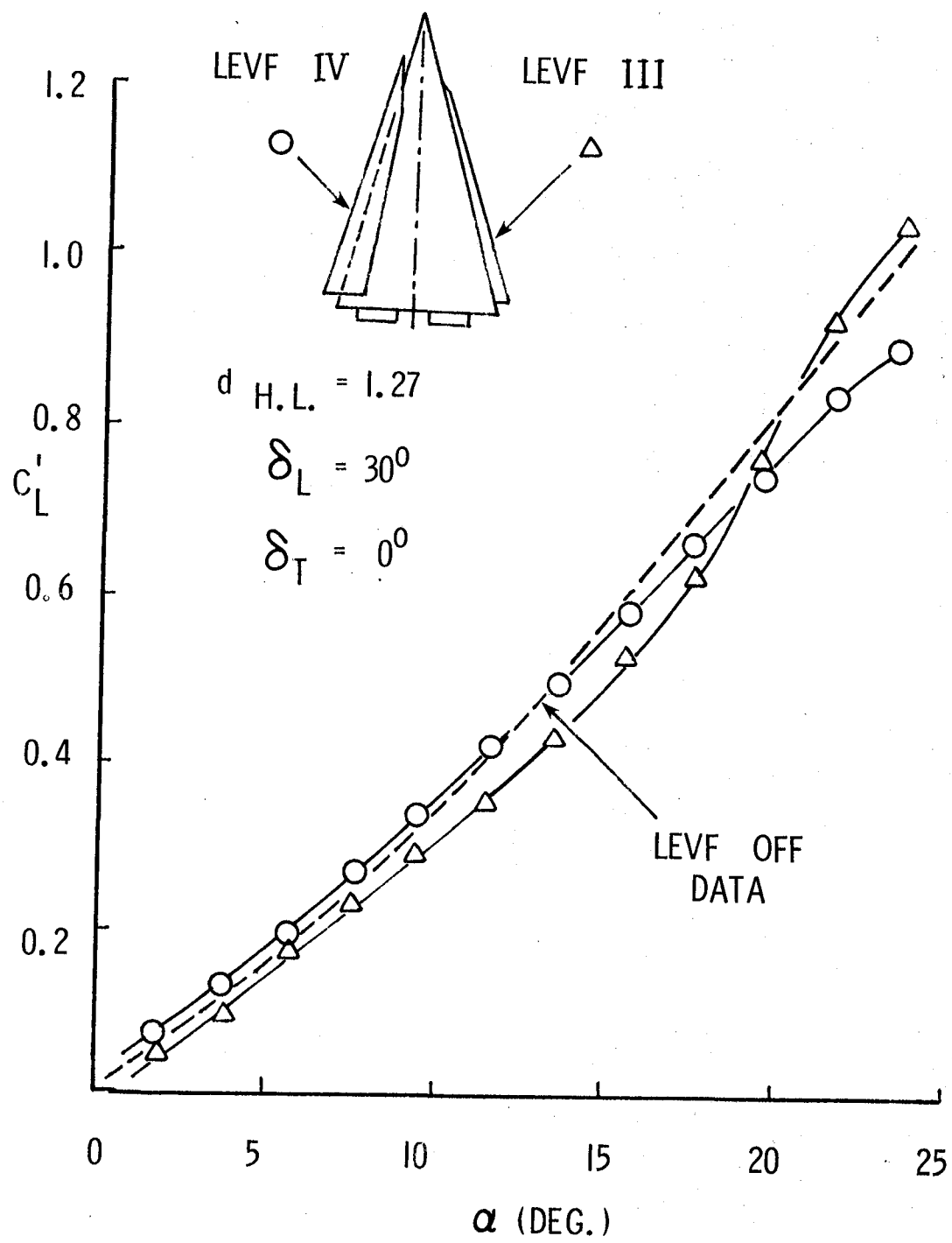


FIG. 13 B COMPARISON OF INVERSE-TAPER AND EXTENDED FLAP AREA-CORRECTED LIFT CHARACTERISTICS

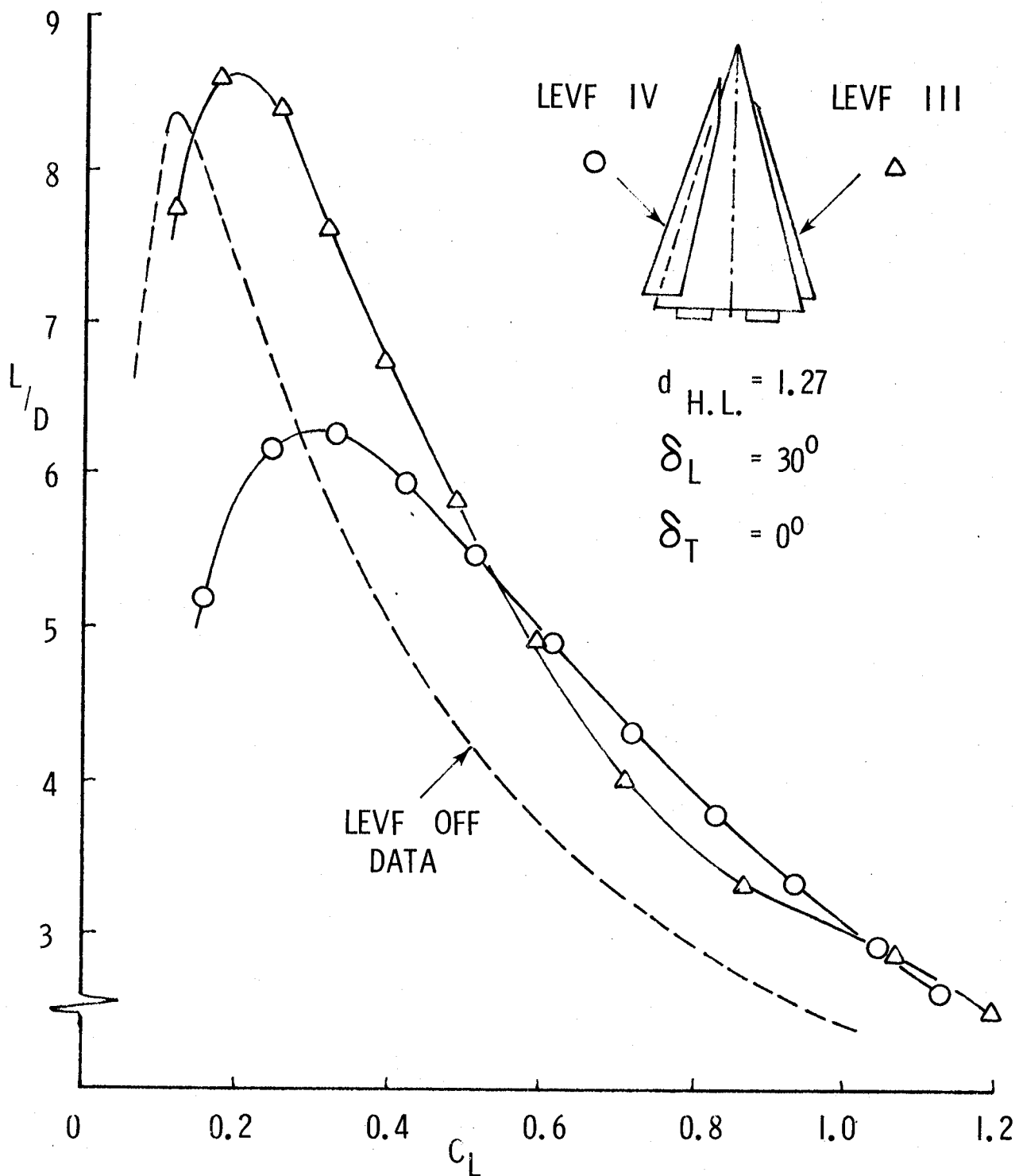


FIG. 14 A COMPARISON OF INVERSE-TAPER AND EXTENDED FLAP  
L/D VS.  $C_L$  CHARACTERISTICS

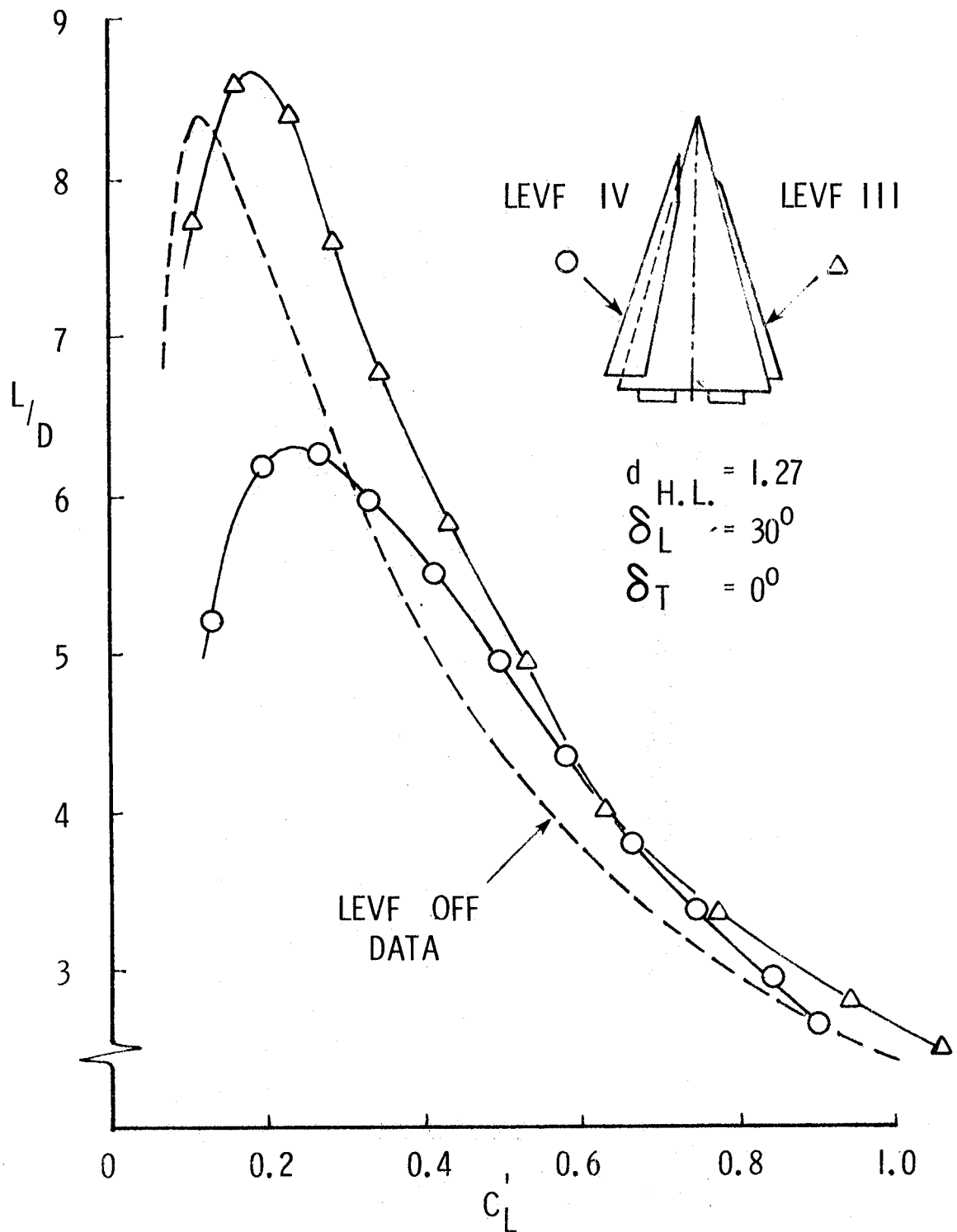


FIG. 14 B COMPARISON OF INVERSE-TAPER AND EXTENDED FLAP  $L/D$  VS.  $C_L$  (AREA-CORRECTED) CHARACTERISTICS

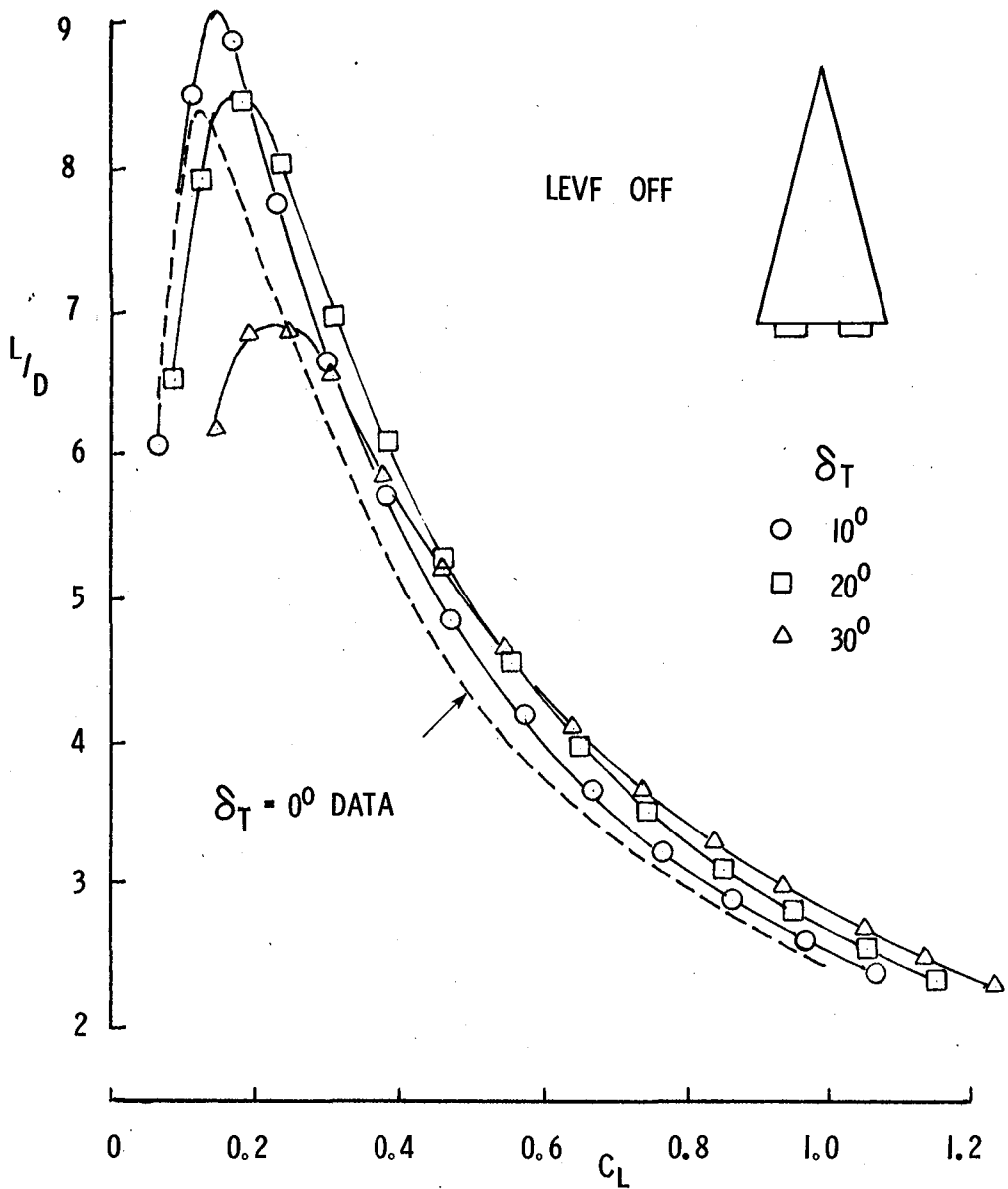


FIG. 15 EFFECT OF TRAILING-EDGE FLAP DEFLECTION ON  
L/D VS.  $C_L$  CHARACTERISTICS -- LEVF OFF

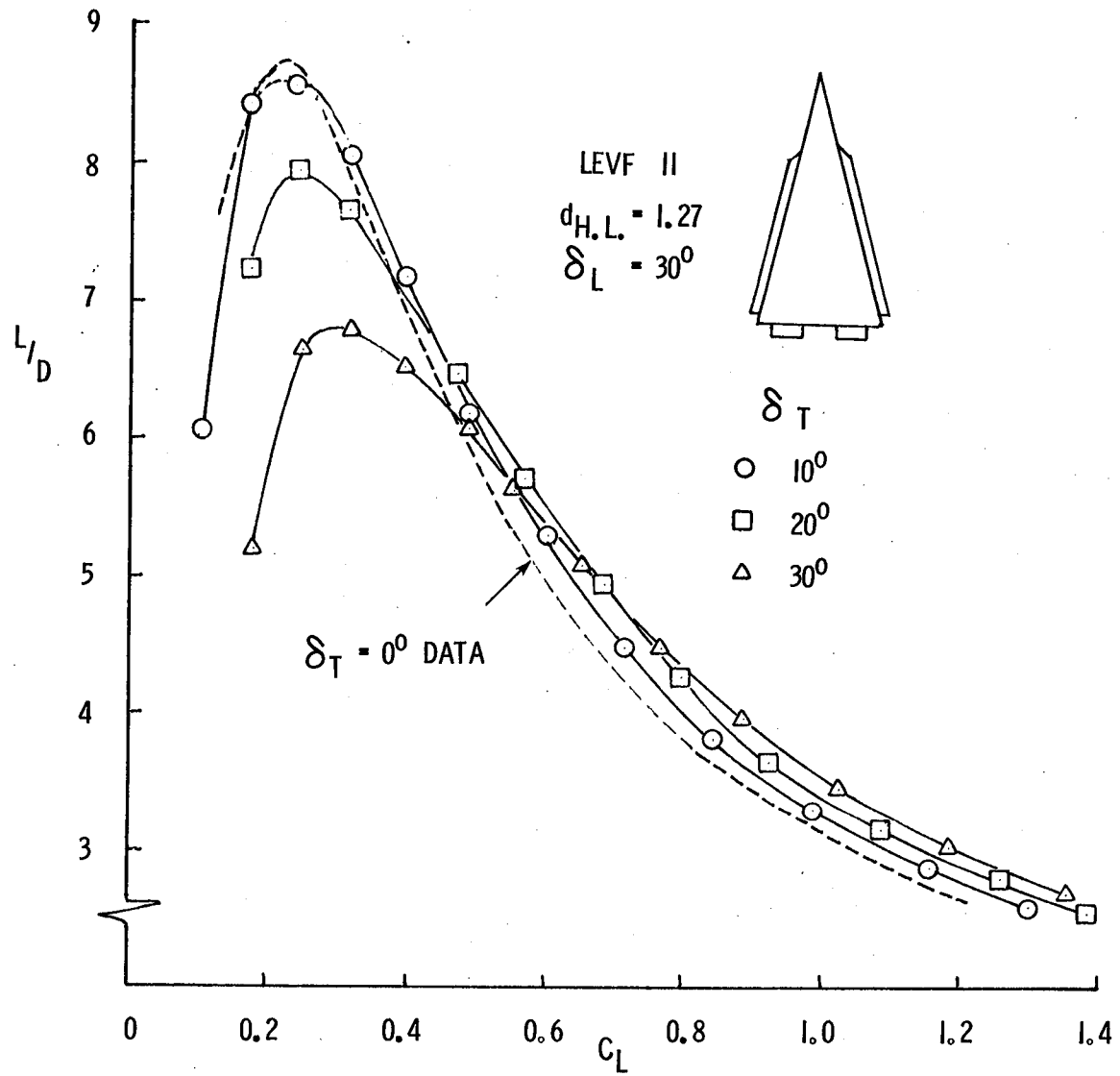


FIG. 16 EFFECT OF TRAILING-EDGE FLAP DEFLECTION ON  
 $L/D$  VS.  $C_L$  CHARACTERISTICS -- LEVF ON

$$d_{H.L.} = 1.27 \quad \delta_L = 30^\circ \quad \delta_T = 30^\circ$$

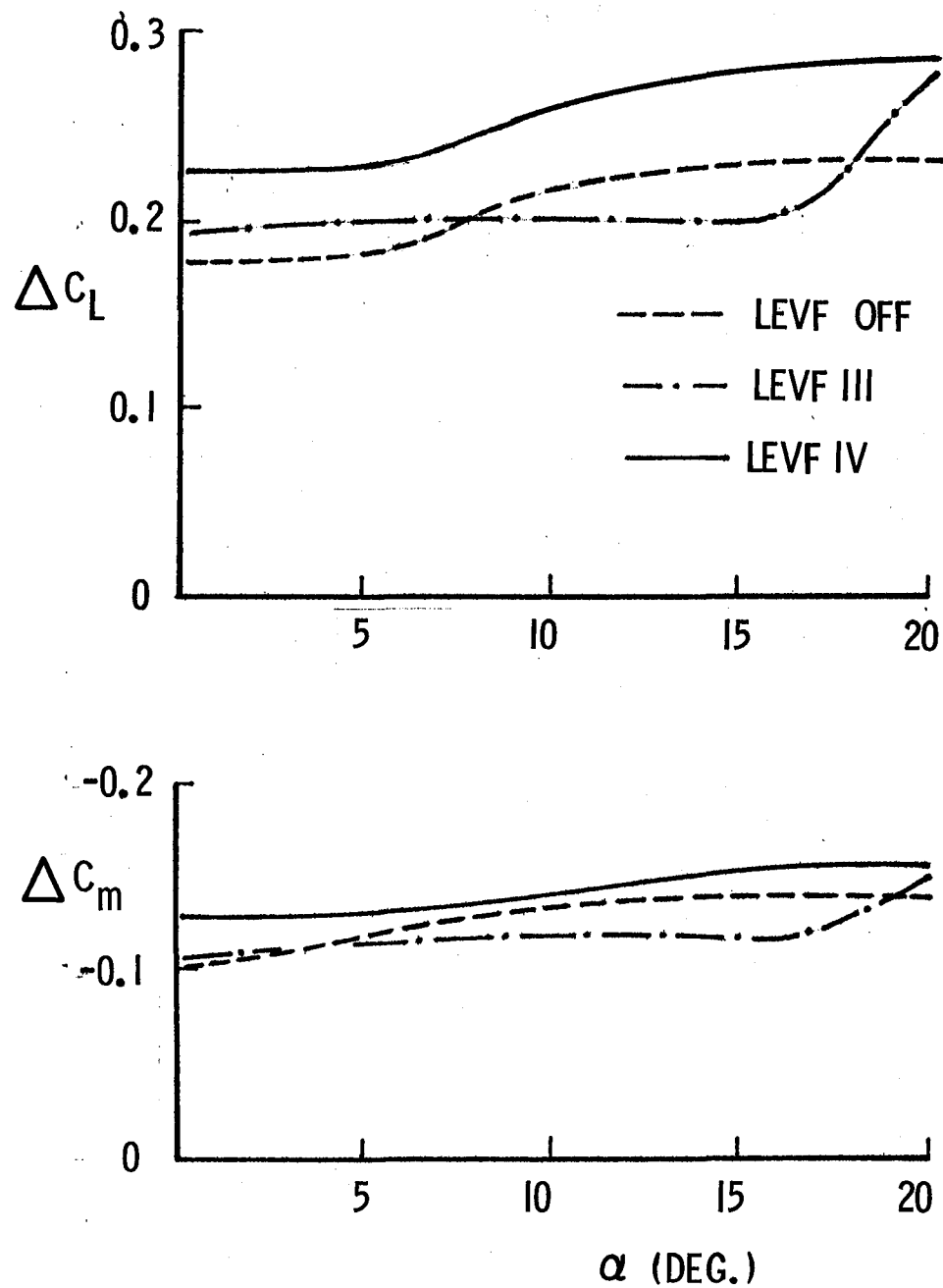
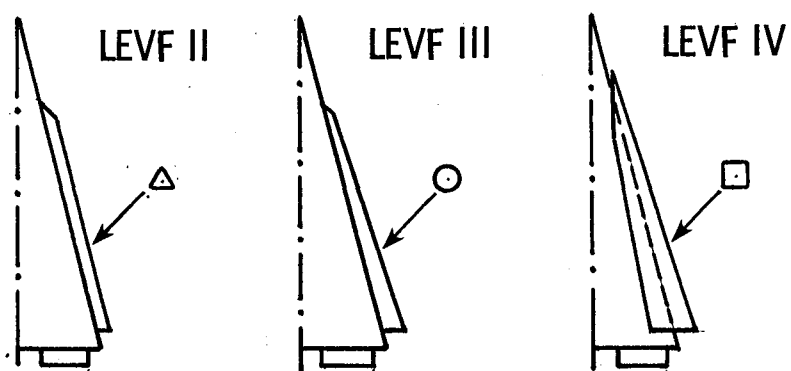


FIG. 17 LIFT AND PITCHING-MOMENT INCREMENTS AT  
 $30^\circ$  TRAILING-EDGE FLAP DEFLECTION



$$d_{H.L.} = 1.27; \delta_L = 30^\circ; \delta_T = 0^\circ.$$

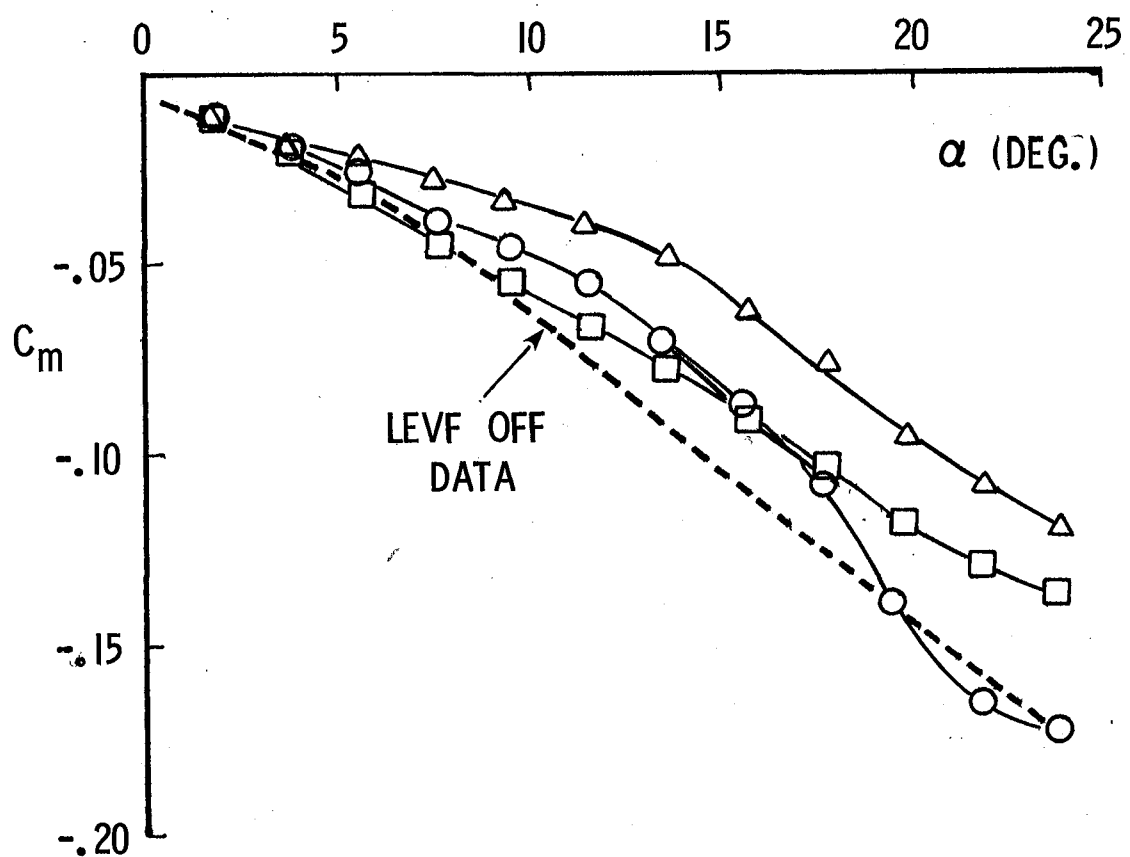


FIG. 18 COMPARISON OF PITCHING-MOMENT CHARACTERISTICS OF VARIOUS LEVF CONFIGURATIONS

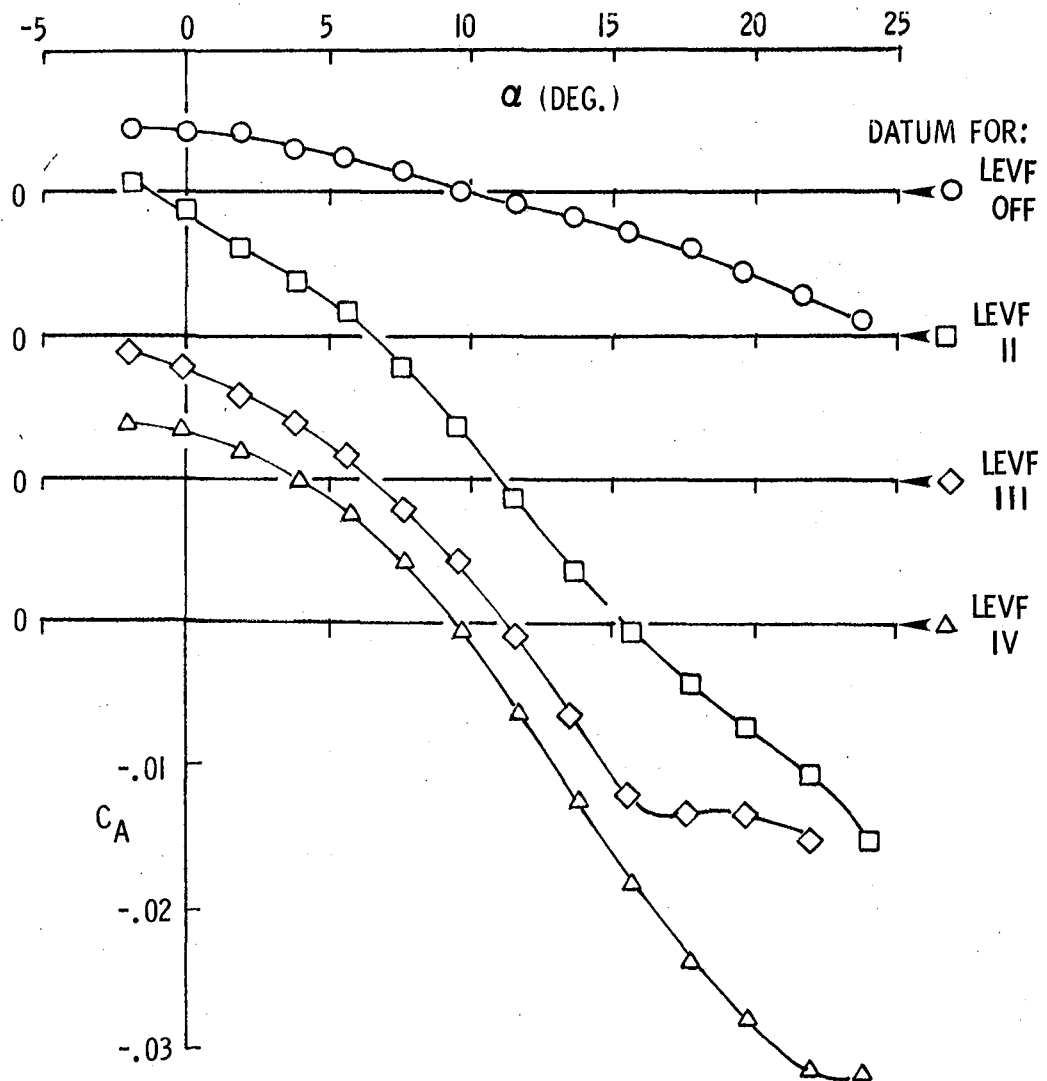


FIG. 19 AXIAL FORCE VS. ANGLE OF ATTACK CHARACTERISTICS

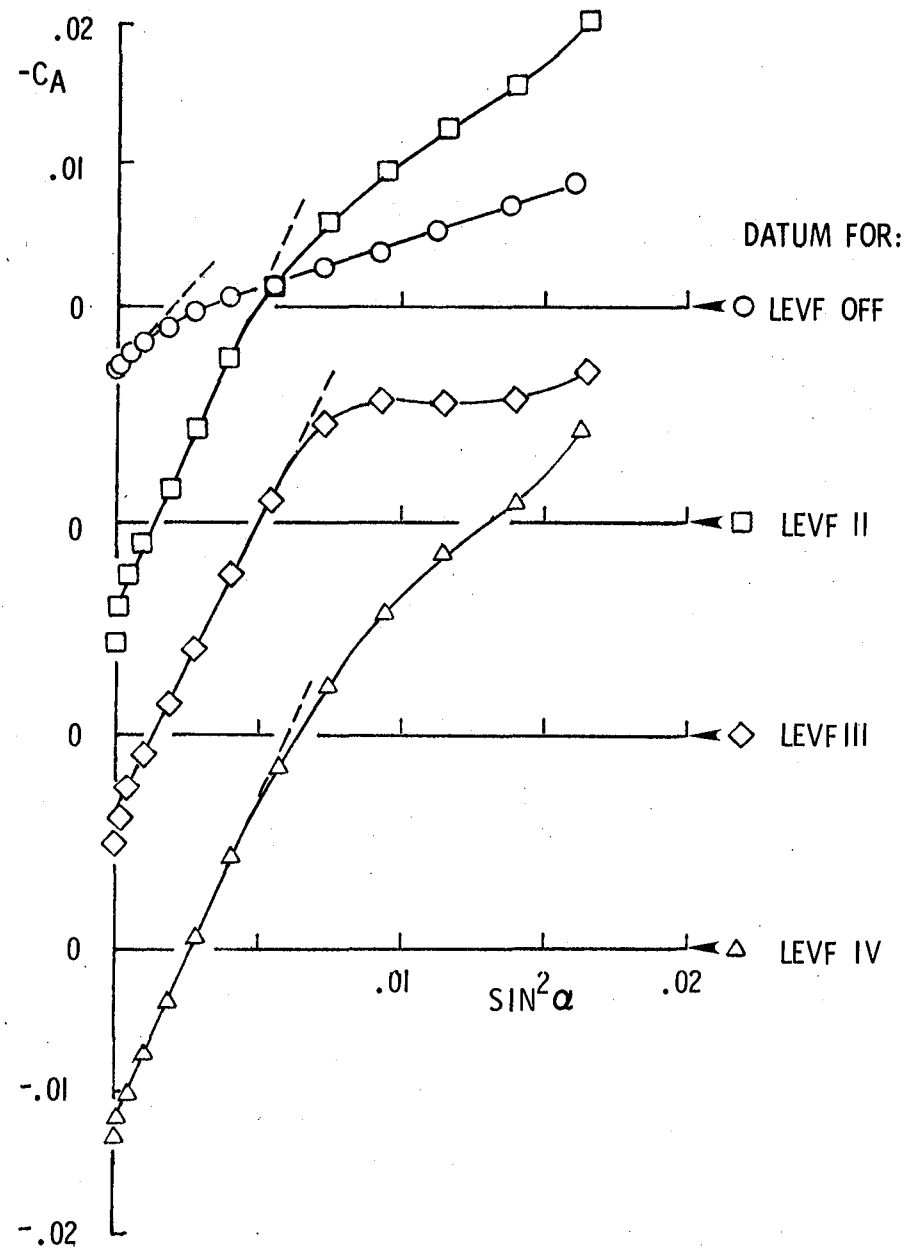


FIG. 20 AXIAL FORCE VS.  $\sin^2 \alpha$  CHARACTERISTICS

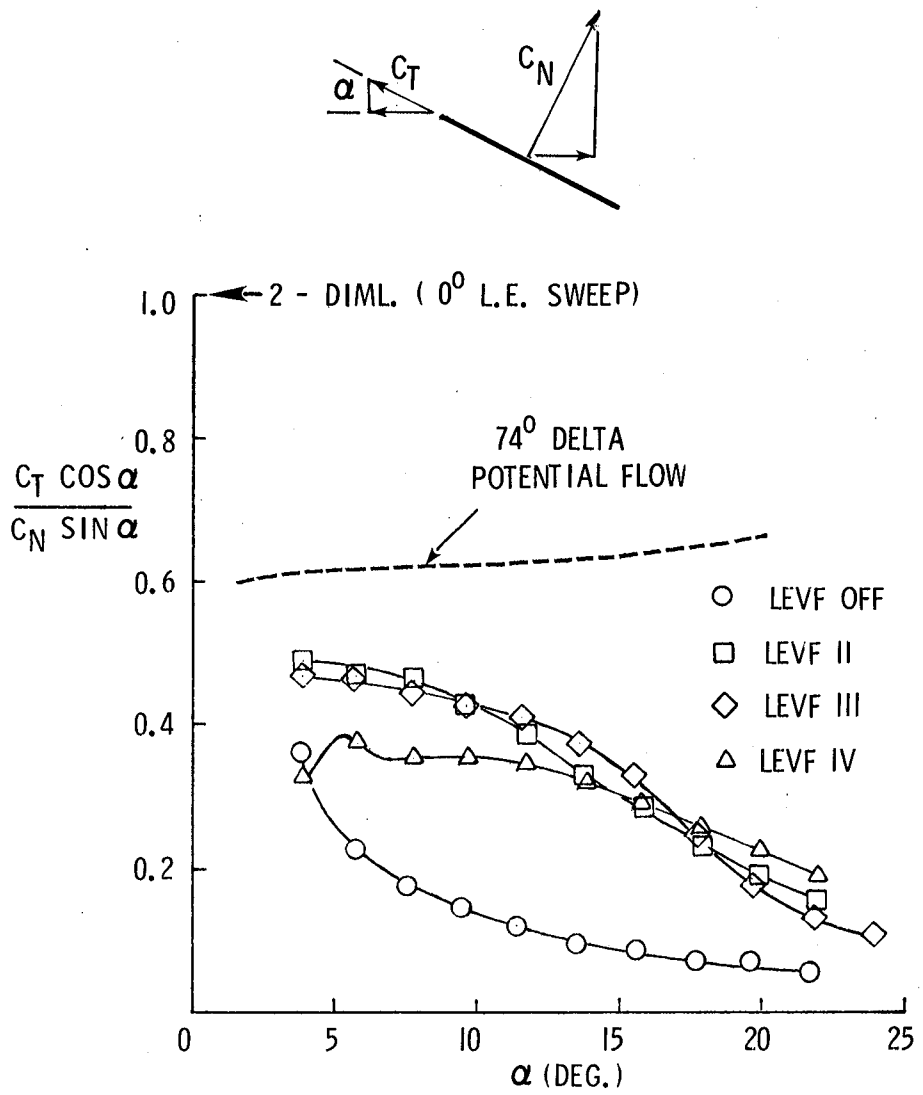
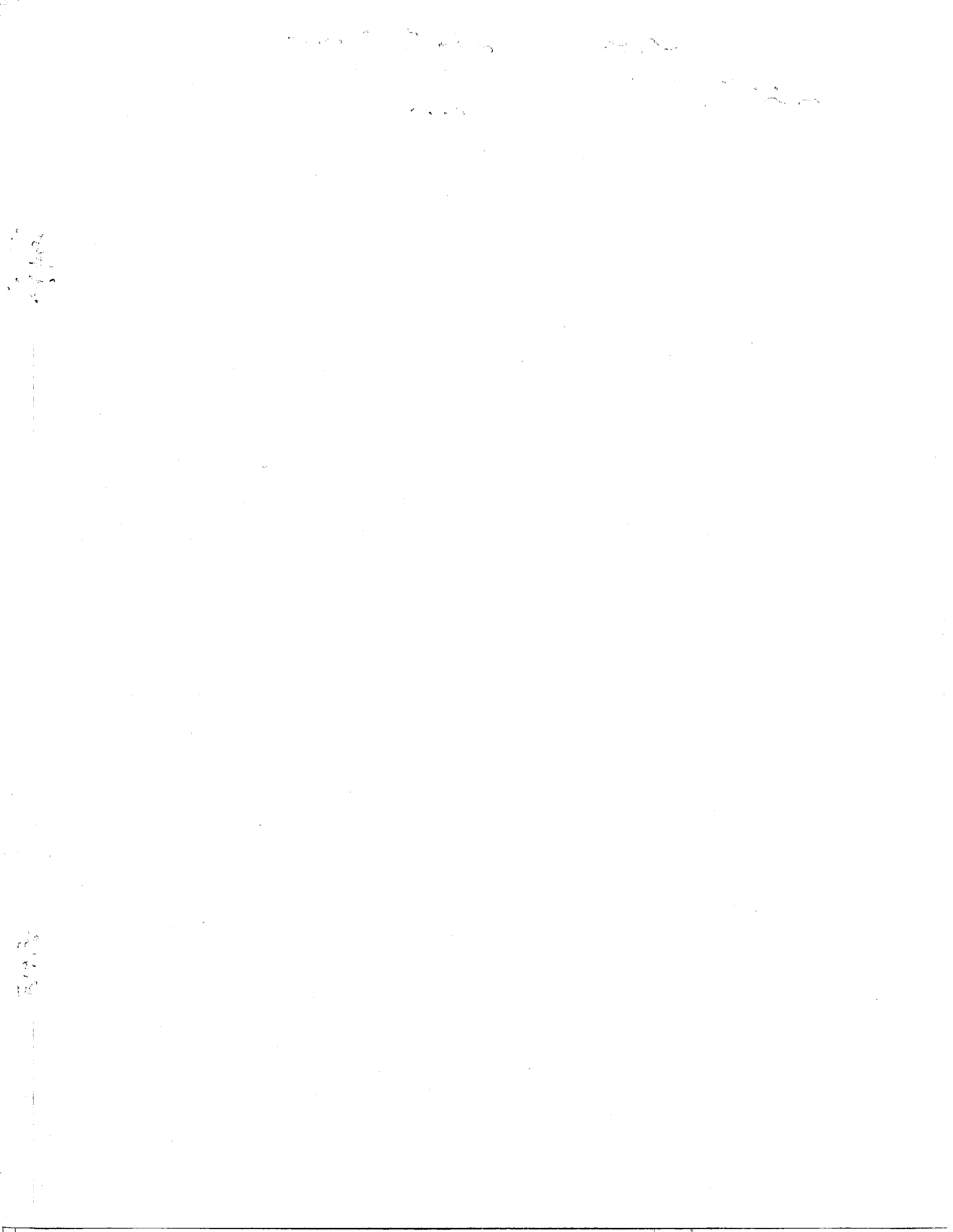


FIG. 21 L.E. THRUST PARAMETER VS. ANGLE OF ATTACK





**DO NOT REMOVE SLIP FROM MATERIAL**

Delete your name from this slip when returning material  
to the library.

NAME	DATE	MS
K. Nodderer	12/23	189
C. P.	1/1/91	201
Linda Pack	10/02	170

NASA Langley (Rev. Dec. 1991)

RIAD N-75